Journal of Sustainable Metallurgy (2021) 7:1483–1505
https://doi.org/10.1007/s40831-021-00428-1

THEMATIC SECTION: MINE TAILINGS: PROBLEM OR OPPORTUNITY? TOWARDS A COMBINED REMEDIATION AND RESOURCE RECOVERY APPROACH

Physical–Chemical Characterization of the Neves Corvo Extractive Mine Residues: A Perspective Towards Future Mining and Reprocessing of Sulfidic Tailings

Alexandra Gomez Escobar[1] · Jorge M. R. S. Relvas[1] · Álvaro M. M. Pinto[1] · Mafalda Oliveira[2]

Received: 31 May 2021 / Accepted: 11 August 2021 / Published online: 14 September 2021

Abstract

Neves Corvo is an underground high-grade Cu–(Sn)–Zn mine, located in the Portuguese part of the world-class Iberian Pyrite Belt (IPB), which is currently producing copper, zinc, and lead concentrates. The operation is owned by SOMINCOR, a subsidiary of Lundin Mining, with a maximum capacity of 2.6 Mtpy for the copper processing plant and 1.0 Mtpy for the zinc processing plant. From 2010 till end of 2019, the mine has accumulated 7.3 Mt of waste rock and 17 Mt of thickened tailings. These mining residues are stored in Cerro do Lobo Tailings Management Facility (Cerro do Lobo TMF), which completes a volume of 47 Mt since the beginning of the operation in 1989 (30 Mt are slurry tailings). The deposition method changed in 2010 from slurry subaquatic deposition to sub-aerial thickened tailings stack (vertical expansion) in co-deposition with potentially acid-generating (PAG) waste rock. X-ray fluorescence analysis have shown copper and zinc grades variation in the waste rock between 0.12 and 0.4%, and 0.1% and 0.3%, respectively, and concentrations up to 0.6% and 1.3% of copper and zinc, respectively, in the tailings. Mineralogically, the tailings consist mainly in pyrite, sphalerite, chalcopyrite, ± arsenopyrite, ± tetrahedrite-tennantite, and gangue minerals such as quartz, phyllosilicates, carbonates, and some oxides, and have a non-uniform particle size distribution ranging between 1 and 100 µm. The waste rock fraction is millimetric to centimetric in size and is formed by the local host rocks, mineralogically consisting in quartz, chlorite (clinochlore and chamosite), calcite, and variably abundant disseminated sulfides, largely dominated by pyrite. Both mining residues might be envisaged as materials with valorization potential both for base metal recovery (tailings) and/or as non-metallic raw materials for construction or other applications (waste rock).

The contributing editor for this article was Max Frenzel.

✉ Alexandra Gomez Escobar
agescobar@fc.ul.pt

[1] Faculdade de Ciências, Instituto Dom Luiz, Universidade de Lisboa, Lisbon, Portugal

[2] SOMINCOR-Lundin Mining, Neves Corvo Mine, Castro Verde, Portugal

Graphical Abstract

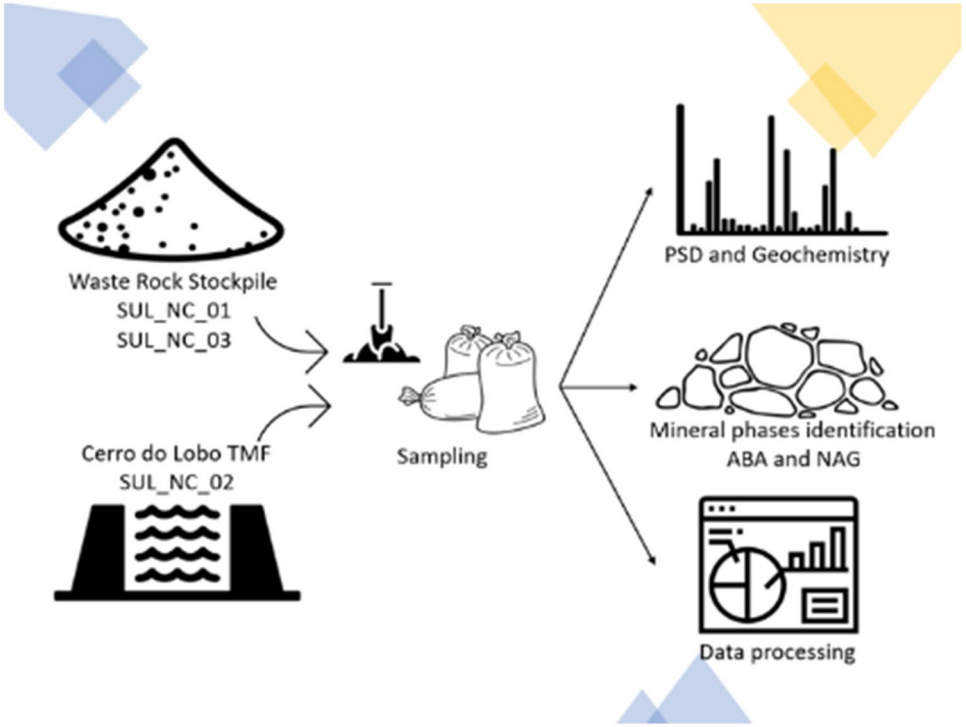

Keywords Neves Corvo mine · Tailings · Waste rock · Ore characterization · Future mining

Introduction

Despite its small territory, Portugal has a high geological and geodynamic diversity, responsible for high metallogenetic potential for a significant variety of ore types, which has generated in the past, and still does, considerable interest for the mining industry. As a consequence, besides three active mines – Panasqueira (W-Sn), Neves Corvo (Cu–Zn) and Aljustrel (Zn-Cu)—Portugal has a relevant mining legacy, especially as a result of the post-industrial revolution period, when mining assumed a good position at economic scales in the country [1]. However, in result of poorly regulated environmental concerns during much of that time, there are now a significant number of abandoned mine sites spread all around the country, most of them from ancient exploitation of basic and precious metals, as well as tungsten, uranium, lithium, and a little bit of coal [2]. The lack of closure plans, waste management and remediation of tailing facilities led to many degraded mining areas, 175 of which inventoried by the Portuguese public company *Empresa de Desenvolvimento Mineiro -EDM-* [3]. Most abandoned mine sites in Portugal correspond to waste piles comprising waste rock, tailings, slags, and mine water resulting from metallic operations with high potential to Acid Mine Drainage (AMD) generation [1, 4]. The identification of these issues and the need in finding suitable means for the recovering and environmental remediation of these areas was the main basis for specific Portuguese legislation in 2001 (Decree Law No. 198-A/2001). By 2015, 95 heavily impacted mining areas have already been recovered by EDM, and some more are on process of remediation. Similar histories and scenarios could be described in many other places worldwide, particularly in the European continent [5].

It is known that operations in the mining industry include mining (exploitation), mineral processing, and metallurgical processes. All three of these principal activities produce solid, liquid, and gaseous wastes [6] called either mine waste or tailings depending on the stage of the process. The waste generated by mining operations has different physical and chemical properties; for example, their volume varies depending on the mining method and type of raw material, and their chemical composition depends on the type of ore, geological settings, and beneficiation process [7]. Therefore, mining produces large quantity of waste [6, 8, 9] and its production has grown dramatically over the last century [10]. With an expanding world market for mineral commodities, mining companies are exploiting lower grade ore bodies [9], implying that increasingly larger quantities of waste rock

and tailings are produced. Recent estimates indicate that production of mine tailings in the world can go up to five to fourteen billion tons per year [11, 12]. Today, mining, and quarrying waste production represents the second largest rate, at 28% of the total waste volume generated in the EU27 countries, preceded only by construction and demolition industry [13]. Some mining operations can generate tailings that represent around 97 to 99 percent of the total ore processed [14], which is why tailings and mine waste management has become one of the main issues addressed in the mining industry. The poor management of these residues, especially sulfidic tailings, do represent not only a significant environmental hazard [1, 15], but also a spatial and engineering challenge sometimes with massive technical and economic implications [16].

Another major issue involving mine wastes and tailings is that these residues are often poorly characterized as a potential mineral resource. In fact, few years ago the South African code for the reporting of exploration results, mineral resources, and mineral reserves -SAMREC (2016)- followed by the "Committee for Mineral Reserves International Reporting Standards -CRIRSCO (2019)- have suggested the following definition of mineral resource: *"The term Mineral Resource covers in situ mineralization as well as residues, low grade stockpiles or tailings that have been identified and estimated through exploration or assessment and sampling…"*. These documents establish that with the proper characterization methodology, resources and reserves can be estimated from mine sites and tailings facilities as they become an economic interest for the companies and a possible source of metals: *"If some portion of stope-fill or stockpile, residue or low-grade stockpiles, remnants, pillars and tailings is currently sub-economic, but there is a reasonable expectation that it will become economic, then this material may be classified as a Mineral Resource"* [17, 18]. So, high demand for minerals in the industry and society's appetite for commodities have changed the mining business in favor of critical raw materials (CRM) and secondary raw materials that can result from the recovery and reprocessing of extractive waste [1, 12], especially in cases where those raw materials, although economically important for the European economy, have their supply dependent on third parties with high associated risk [15]. Furthermore, many metals, which are by-products of base metal production and did not have significant application in past years, are now used in new, high-tech, and green technologies, which have increased their net value; however, their known reserves are still very limited and/or poorly constrained [19].

Recently, the European Innovation Partnership (EIP) on Raw Materials launched a "call to arms" to transform the "extractive waste problem" into a "resource-recovery opportunity" [20]. In order to develop a highly skilled workforce to mitigate environmental risks and to economically recover valuable raw materials, the European Training Network (ETN) for the remediation and reprocessing of sulfidic mining waste sites (SULTAN project) provides the first-ever training program dedicated to the reprocessing of tailings.[1] By integrating active mines and abandoned tailings ponds in its approach, this project challenges the scientific community and the various stakeholders to question whether the mines actually end their productive life after the shutdown of the exploitation operation of its primary resource. A circular exploitation strategy (following the circular loop of Refuse, Reform, Reduce, Reuse, Recycle with a final destination with minimum waste), is increasingly adopted at the early stages of any resource's life cycle assessment. One of the goals of the SULTAN project, through the Faculty of Sciences of the University of Lisbon, Portugal, focuses on the geometallurgical characterization of (i) Cerro do Lobo Tailings Management Facility (TMF), and (ii) of its three types of mine residues: fresh waste rock (SUL_NC_01), tailings (SUL_NC_02) and stored-oxidized waste rock (SUL_NC_03) in order to identify possible valuable metals (Cu, Zn, Pb) and by-products (*e.g.*, In, Se, Ag) for reprocessing and valorization (on-going research performed by the various SULTAN partners). Figure 1 illustrates the different mining operations from where each of these materials is obtained. SUL_NC_01 represents the crushed waste rock coming out of the underground operations that could not be used in the backfilling process; SUL_NC_02 consists of the composite material resulting from the mixture of copper and zinc processing plant tailings, and SUL_NC_03, represents oxidized waste rock that have been stored in a stockpile for around 30 years, since the beginning of the mining operations. All the three materials have a final disposal at the Cerro do Lobo Tailings Management Facility (TMF).

Taken as a whole, the high variability of physico-chemical characteristics of tailings represents a wide set of geochemical, geotechnical, and environmental challenges [21], which define their physical and chemical behavior and, therefore, the potential environmental footprint of such materials and their optimal disposal methods. Here, we present the physical–chemical characterization of the Cu–Zn tailings and other mine residues produced at the Neves Corvo mine, taken as a case study representative of an active, large-scale mining operation in Europe. This is part of an on-going broader research that will make use of a holistic view over the whole resource circuit, from mine to TMF, towards a geometallurgical model, to be presented at the end of the project, that might assist in evaluating the potential for future mining and reprocessing of sulfidic extractive mine residues.

[1] https://etn-sultan.eu/sultan-project/

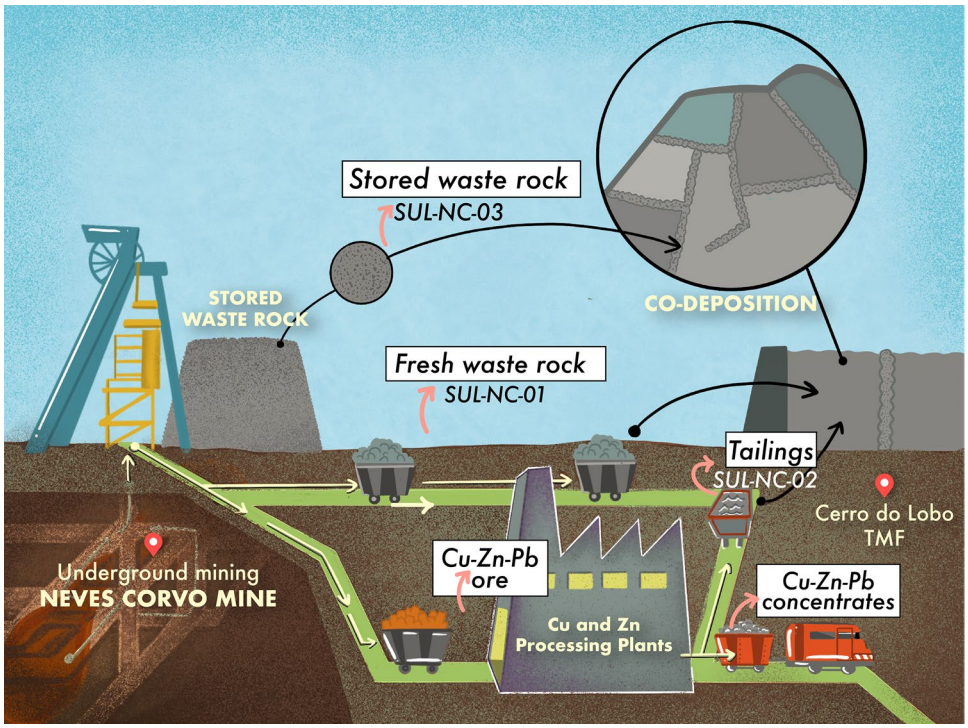

Fig. 1 Types of material sourced by the Neves Corvo mine operation investigated in the course of the SULTAN Project

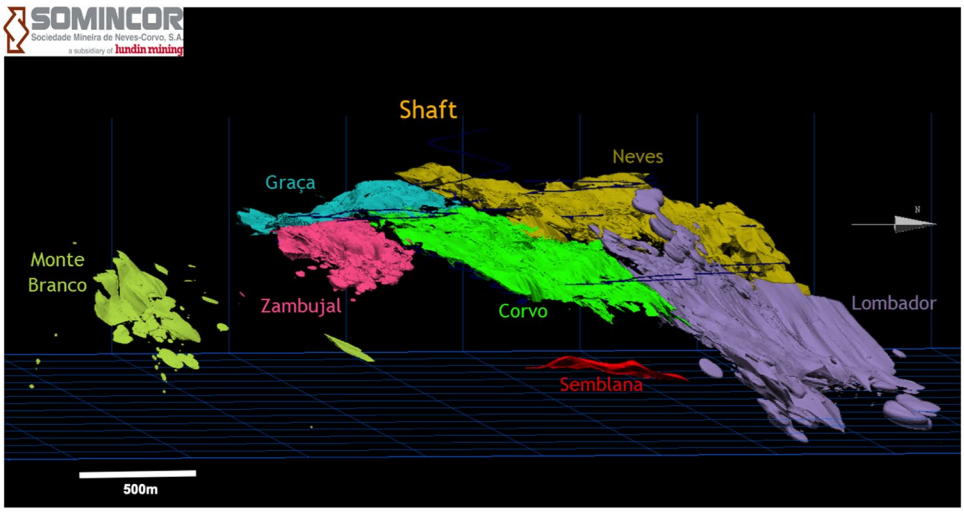

Fig. 2 Neves Corvo orebodies after SOMINCOR, 2019

Neves Corvo Mine: Case Study

Neves Corvo is a high-grade Cu–(Sn)–Zn volcanic-hosted massive sulfide (VMS) deposit located in the Portuguese sector of the Iberian Pyrite Belt, 220 km south of Lisbon, in the district of Beja (Baixo Alentejo province). Underground mining at Neves Corvo started in 1988 and has been continuously conducted, producing copper, tin (now exhausted), zinc and lead concentrates from five massive and stringer sulfide orebodies: Neves, Corvo, Zambujal, Lombador and Graça, the latter being already fully mined. Two other orebodies, named Semblana and Monte Branco, were more recently discovered, in 2010 and 2012, respectively, being still undeveloped (Fig. 2).

Copper production at the Neves Corvo mine has started in 1989, followed by tin production, between 1990 and 2001, and by zinc/lead production in 2006 [22]. Currently, copper, zinc and lead production are carried on two processing plants with a maximum capacity of 2.6 Mtpy for the copper circuit and 1.0 Mtpy for the zinc–lead circuit. In 2020, mineral reserves for the Neves Corvo deposit (proven plus probable) have been estimated to a total of 57.6 Mt, of which

29.7 Mt are classified as copper ores at 2.0% Cu, 0.8% Zn, 0.3% Pb and 30 g/t Ag, and 30.1 Mt are classified as zinc ores at 0.3% Cu, 7.3% Zn, 1.8%Pb and 62 g/t Ag [23]. Estimated copper and zinc resources at Neves Corvo (measured plus indicated) are 61.9 Mt at 2.3% Cu, and 71.3 Mt at 6.9% Zn, respectively [23].

The underground mining operations at the Neves Corvo mine employ several stopping methods, being bench-and-fill and drift-and-fill the most representative. Filling is made with a paste composed by the finer fraction of tailings (< 50 µm) and cement [24]. Underground levels were related to a datum of 1000 m below sea level, while the mine surface elevation is approximately at 1220 m above datum [25]. There are two accesses to the underground workings: by shaft (for ore and waste) and by a ramp from the surface (for people and material coming in and out of the mine). The shaft is located to the west of the Corvo orebody; its main use is to transport the ore from the 700 m level to the surface and it is equipped with a double drum winder and two capacity skips. Conveyors are used in deeper levels to transport the ore to the 700 m level [25–27].

Underground operations comprise two crushing stages: (i) the upper ground crusher station, located at the 700 m level, is used to process ore and waste from the Upper Corvo, Neves, Zambujal and the exhausted Graça orebodies, with a 600t/h capacity for the jaw crusher and approximately 1,500t of capacity in storage; and (ii) the secondary crusher station, located at the 550 level, which serves the lower section of the mine, being used to process ore from the Lower Corvo and Lombador orebodies, also with a capacity of 600t/h [25]. Mining activity and production of base metal concentrates in Neves Corvo generates two different types of residues: (i) waste rock, the hosting rock extracted and crushed during mining operations; and (ii) tailings, the final residues from copper and zinc processing plants. More than 60% of the waste rock generated is used directly as waste fill underground, being the remaining fraction crushed and hoisted to the stockpiles at surface. The waste rock occurs in a size fraction ranging from 0 to 200 mm as it comes from underground crushing stages, and consists mainly of variably mineralized felsic volcanic rocks and dark shale with sulfides in veins and disseminations [22, 28, 29].

Ore Geology

The Iberian Pyrite Belt (IPB), where the Neves Corvo mine locates, is a widely known metallogenic province in the south of Portugal and Spain, where numerous volcanic-hosted massive sulfide (VMS) deposits occur as massive sulfide lenses commonly clustered in small areas and hosted by a variably thick volcanic sedimentary sequence [30–34]. Neves Corvo stands out in the IPB for its high copper and zinc grades, huge tonnages, and occurrence of uniquely high tin grades in massive and stringer cassiterite ores [29, 35]. The detailed stratigraphy, geochronology and physical volcanology of the Neves Corvo world-class deposit has been object of numerous studies [36–39], while its extraordinary ore-forming processes still fuel some metallogenic debate [29, 40–45].

Table 1 Distribution of ore types at Neves Corvo processing plants

	Copper processing plant	Zinc (and lead) processing plant
Ore types	MC	MZ
	MCZ	FZ
	FC	MP
		MZP

Three different styles of mineralization (massive, fissural and "*rubané*") and at least thirteen ore types have been described at Neves Corvo: 1-the massive sulfide mineralization includes copper (MC), tin (MT), copper-tin (MS), zinc (MZ), copper-zinc (MCZ), lead (MP) and zinc–lead (MZP) ores; 2-the fissural (or stockwork) mineralization includes copper (FC), tin (FT) and zinc (FZ) stockwork ores; and lastly, 3-the "*rubané*" mineralization (banded ores, named after the French word, consisting in fact in sheared stockwork mineralization tectonically emplaced on top of the massive sulfide lenses; [29] includes copper (RC), tin (RT) and zinc (RZ) ores [22, 43]. The various types of *"rubané"* ores, as well as the massive and stringer cassiterite ores (MT, FT) are now exhausted.

The ore mineralogy at the Neves Corvo deposit comprises major, minor and trace minerals, including native gold, bismuth, and a variety of lead, copper and tin sulfosalts, and cobalt and arsenic sulfides and selenides, [1, 46–48]. Pyrite is by far the most abundant sulfide mineral, often associated to sphalerite, galena, chalcopyrite and arsenopyrite [28]. Minor amounts of tetrahedrite, tennantite, stannite, cassiterite, kesterite and pyrrhotite can be found filling spaces in pyrite grains or replacing pyrite. The most common gangue minerals are quartz, chlorite, sericite, and carbonates (mostly siderite and ankerite) [28, 46, 48, 49].

Mineral Processing-Ore Beneficiation

At present, the Neves Corvo mine has two operative processing plants: one for copper and one for zinc (and lead). The copper processing plant has an annual capacity of 2.6 million tons per annum (mtpa), and the zinc processing plant has a capacity of 1.1 mtpa [24]. Copper and zinc concentrates leave the mine transported by train to SOMINCOR's port located in Setubal municipality and are further shipped to a variety of commercial smelters in Europe. Lead concentrate is stored in containers and taken to maritime ports [24].

Following the previously described underground crushing stage, the material is sorted as a function of the ore types and distributed to the copper and zinc processing plants (Table 1). Then, the main sequence of operations followed at the processing plants comprises secondary and tertiary crushing, grinding, flotation and thickening. At the end of the crushing and grinding stage, materials are classified in a closed circuit to be returned to grinding stage if material is still too coarse, whereas the fines follow to a flotation stage and finally to a thickening stage. The products that result from a previous stage feed the next one [50].

The main concentration process both at the copper and zinc processing plants is flotation, which follows crushing and grinding stages and precedes the final thickening phase. At the copper processing plant, two concentrates are produced: copper and zinc, being zinc a by-product obtained from the complex ores, where copper and zinc sulfides occur together (MCZ). The zinc processing plant also produces two concentrates: lead and zinc as main products. The end of the zinc circuit requires an IsaMill stage to reduce particle size to very fine-grained material (< 20 μm) in order to liberate finer particles going through another flotation circuit. Some of the concentrates are sent to a cleaning flotation stage to obtain a higher recovery of metals [50].

Tailings from both processing plants are mixed and the composite is pumped to the Cerro do Lobo Tailings Management Facility (TMF) just as it comes out of the concentration processes, always that the coarser fraction is not needed for paste filling in the mining operations. When this is the case, the mixed tailings are classified by size using hydrocyclones, and only the finer fraction is pumped to the Cerro do Lobo TMF.

Tailings Disposal at Cerro do Lobo Tailings Management Facility (TMF)

Since the beginning of the mining operations at Neves Corvo, the tailings dam was designed to held originally 17.5 M m^3 of tailings using a sub-aqueous disposal method through pipelines coming from the processing plant and spaced 100 m each from the main embankment, in order to distribute evenly the material. The Cerro do Lobo TMF is delimited by a conventional clay-cored rockfill embankment, 3.3 km long, 42 m height and with an approximate area of 190 ha. The original embankment has been modified three times using the downstream dam construction method to guarantee the storage capacity needed in each stage of development of the mining operation [51].

Considering that about 90% of the mill tailings are heavy metal-bearing sulfides it was required to design an environmentally safe disposal system that might kept simultaneously opened the possibility of recovery of residual values in copper, zinc, and tin in some point in the future [52]. The capacity of the Cerro do Lobo TMF as it was originally designed would have reached its threshold in 2011, shortening the lifetime of the mine in 15 years; by that time the mine reserves were estimated to last until 2026. A 10-year-long research project was carried out seeking a solution for a suitable disposal method for the mine. By the end of 2010, the tailings storage process was finally converted to sub-aerial deposition using thickened tailings in a co-deposition system with containment berms built with waste rock [51]. Waste rock is temporarily stored in a stockpile located at the north of the mining complex. The tailings are pumped and disposed flowing according to ground's slope, until it stabilizes. Later on, the layer starts its consolidation process, releasing the water downstream the layer's slope. Based on the pilot plant and experience in management of Neves Corvo tailings, keeping the material free of water avoids oxidation and possible events like liquefaction, infiltration or slipping within the facility [53].

Sub-aerial disposal presents many advantages such as minimizing environmental impacts (less sulfide oxidation and leaching residues), optimizing the geotechnical, geochemical, and hydrogeological stability of the tailings dam and allows the co-deposition with waste rock, which increases the capacity of storage and prevents modifications of the embankment. Between 2010 and 2019, the Neves Corvo operation has accumulated 7.3 Mt of waste rock (SUL_NC_01), which were stored at the Cerro do Lobo TMF together with 17 Mt of thickened tailings (SUL_NC_02), while 3.1 million tons of waste rock remained in a temporary stockpile (SUL_NC_03).

Tailings and Mine Waste: Physico-Chemical Characterization

Sampling, Analytical Procedures and Methods

The materials that are object of this study refer to two types of mine residues—waste rock and tailings—and the sampling plan designed includes three different sets of samples: (i) sampling of fresh waste rock (SUL_NC_01),(ii) sampling of stored waste rock (SUL_NC_03); and (iii) sampling of tailings at Cerro do Lobo TMF and processing plants (SUL_NC_02).

Sampling of Waste Rock Stockpile

The study of old and fresh waste rock was based on a sampling campaign that was ran, respectively, at a stockpile located in the mining complex (SUL_NC_03), and at a disposal point at Cerro do Lobo TMF (SUL_NC_01). Both

Fig. 3 Different colors shown by the old waste rock material, as they can be seen "in situ" (left) and after drying the corresponding samples (right)

materials consist of run-of-mine (ROM) residues resulting from the primary crushing underground. The difference between these two waste materials lies on their storage time: while SUL_NC_01 was picked up on the exact day the material was carried out from the mine, SUL_NC_03 has collected from a stockpile where material has been kept for a period of 25 to 30 years after its underground extraction during an early stage of the mine's life. During this time period, mineral processing operation has been changed several times, including major changes associated to the startup of the zinc processing plant in 2001.

At the stockpile, two tons of SUL_NC_03 were collected and mixed from four different positions: bottom, top, eastern, and western flank, crosscutting the different oxidation layers in order to guarantee the representativity of the material. At the mine waste disposal point at Cerro do Lobo TMF, two tons of SUL_NC_01 were taken from the pile as it came out of the mine, splitting the material homogeneously with a backhoe until a $1m^3$ container was filled. Both samples were sieved in situ at 25 mm mesh, (oversized rocks used as aggregates), homogenized, and split into 10 sub-samples weighting 25 kg each, the remaining material being stored indoors for future use, if needed.

As a consequence of the long exposure to weathering effects of the old waste rock (SUL_NC_03), different layers of oxidized material, showing contrasting colorations, are visible in the stockpile (Fig. 3). Samples of different layers at the stockpile (black layer (SUL_AGE_01W) reddish (SUL_AGE_05W), grayish (SUL_AGE_03W), yellowish (SUL_AGE_02W) and finally, the whitish layer (SUL_AGE_04W)) were taken both for X-ray diffraction (XRD) and for X-ray fluorescence (XRF) analysis, in order to compare the composition and mineralogy of each layer. Samples were dried in an oven at 40 °C for 16 h to remove humidity, split in a riffle until individual samples weighting 60 g were obtained, and powdered in a tungsten ring mill as preparation for XRF analysis.

Sampling of Cerro do Lobo Tailings Management Facility

Cerro do Lobo impoundment is divided into areas where tailings were (and are) progressively disposed following a sequence of filling, compaction, drainage of water and gradual covering, which allowed to sample separately the material disposed in October 2019, in March 2019, and in 2014.

Sample no 1 (SUL_AGE_01T) was taken on the western flank of the impoundment from the discharge point in October 2019; sample no 2 (SUL_AGE_02T) was taken from the cell were tailings were disposed in March 2019; and samples no 3 and 4 (SUL_AGE_03T and SUL_AGE_04T) were taken from the southeastern sector of the dam, corresponding to material already stored for 5 years: sample 3 (SUL_AGE_03T) was collected at the border of the cell, whereas sample 4 (SUL_AGE_04T) was picked up at the center of the cell (Fig. 4).

Sampling of tailings was performed by collecting about 1 kg of blended material of 50 cm-deep holes. All samples were dried at 40 °C for 16 h and split into smaller sub-samples for XRD, laser diffraction and XRF analyses. A complete drilling campaign (CPTu), covering the whole sectors of the impoundment, is now under progress by initiative of SOMINCOR-Lundin Mining. In a further step of this ongoing research, these drill holes, which extend down to the bottom of the impoundment, will allow the in-depth characterization of the tailings stored at the Cerro do Lobo TMF and its evolution through time.

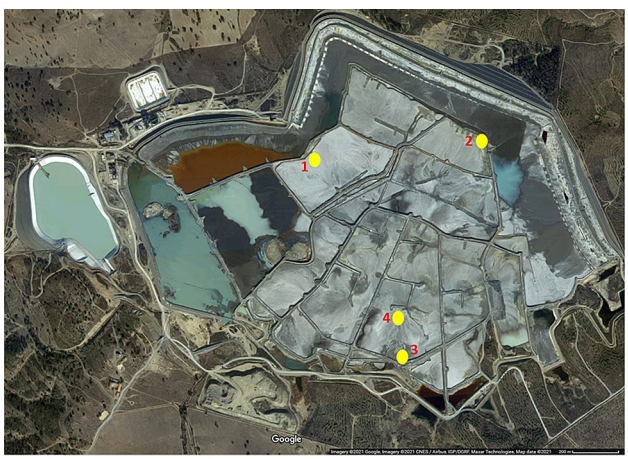

Fig. 4 Sampling points at Cerro do Lobo Tailings Management Facility

Particle Size Distribution and Grindability Optimum Time

As mentioned above, the samples SUL_NC_01 and SUL_NC_03, (fresh waste rock and old waste rock, respectively) were sieved in situ at 2.5 cm, which means that the starting material was still too coarse for any reprocessing method or for further analysis. In order to treat separately the millimetric particles of the sample, coarser sieving for five samples was done using the following mesh sizes: 8 mm, 4 mm, 2.35 mm and 1.25 mm. Each fraction retained in the different meshes were weighted, powdered in a tungsten mill, and analyzed by XRF. Since there was very little material in the fraction < 1.25 mm, eleven sub-samples were passed through the mesh 1.25 mm in order to get five sub-samples of approximately 1—1.3 kg each, equivalent in weight to the coarser fractions sub-samples. The material below 1.25 mm was then sieved for 15 min in a ROTAP machine, generating sub-samples within the following mesh fractions: 335 µm, 250 µm, 106 µm, 63 µm, 45 µm and 20 µm.

Particle size distribution in 130 samples of the tailings collected daily, between July and October, and in 53 samples of thickened tailings, were analyzed by laser diffraction at SOMINCOR's laboratory. In addition, particle size distribution of tailings either from the Cerro do Lobo TMF, or from the two Neves Corvo processing plants was measured using a Malvern 2000 and a Granulolaser Master 5000 laser diffraction particle size analyzers at the University of Lisbon and at the STEVAL laboratory in Nancy, respectively. A total of 10 samples were measured and taken as representative of the materials studied in this research (control data). As tailings samples are fine powders below 100 µm, no sample preparation was required prior to laser diffraction analysis.

3 sub-samples, weighting 1.3 kg each, of both SUL_NC_01, and SUL_NC_03 waste rock materials, were used to find a grindability optimum time reference equation, by grinding each of them in a ball mill at 15, 22.5 and 30 min. Each ground product was sieved in a ROTAP machine for 20 min with the purpose of getting a granulometric curve corresponding to each grinding time and to estimate the D_{80} of the final product. Then, a linear regression of the data was made for the "time vs. D_{80}" plot, which permitted to obtain the $y = mx + b$ equation required to find the optimum grinding time for any desired particle size.

The experimental "time vs. D_{80}" plot was based on the results obtained from each granulometric analysis after each grinding time, whereas the theoretical "time vs. D_{80}" plot was based on the forecasting of D_{80} values from the cumulative passing percentage calculated.

Geochemistry

A total of 47 samples (30 samples of waste rock, and 17 samples of tailings) were analyzed with a hand-held portable XRF Thermo Scientific NITON XL3t Gold + +, in static mode. The instrument uses an Ag x-ray tube (no radioactive source), with a maximum current of 0.2 mA, a maximum voltage of 50 kV, and a maximum power of 2 watts. All samples were analyzed in a static and closed platform. All the analyses were made in the "Mining Cu/Zn mode" predefined in a library available in the portable system, with all 4 beam times set to 30 s, for a total of 120 s *per* sample, as the instrument operates on four different filters yielding 4 spectra per sample, which provides measurements for 35 elements. The sample preparation before analysis consisted of depositing the powders in sample cups covered with a 6.0 µ thick polypropylene film. To evaluate the accuracy of the XRF analyses, blank duplicates were analyzed randomly. Moreover, whenever possible, the results were compared with high-quality measurements (calibrated) produced at SOMINCOR's XRF laboratory (Fig. 5).

The quality of analytical data produced by portable XRF instruments rely very heavily on careful sample preparation, either in the form of pellets or capsules, to maximize precision and accuracy of the results, which, in addition, are highly improved when the readings are made in static mode inside a dedicated closed platform, as it was the case.

A set of 17 sub-samples were analyzed at ALS Geochemistry for whole rock geochemistry. The analytical methods used were major elements by XRF and ICP-AES; trace elements by Li Borate fusion (fused bead, acid digestion and ICP-MS), four acid digestion and ICP-AES, aqua regia digestion for the volatile trace elements; and total carbon and sulfur by combustion analysis (Leco furnace).

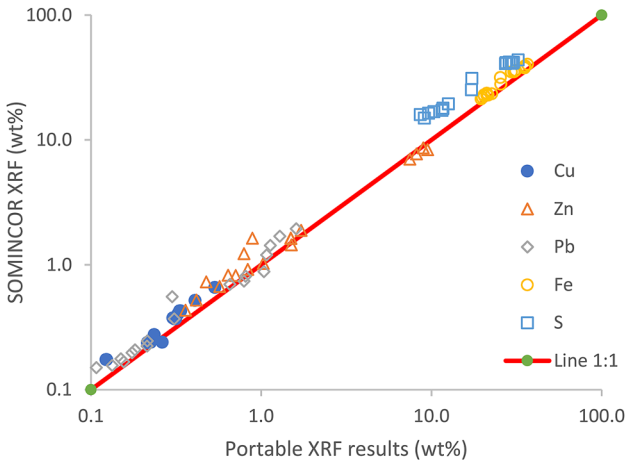

Fig. 5 Portable XRF results vs SOMINCOR -calibrated- XRF Results

Mineralogy

X-ray power diffraction analysis for 3 representative samples of the SUL_NC_01 and SUL_NC_03 waste rock materials were performed at AGQ Mining & Bioenergy laboratory in Spain. The samples were crushed in a disk mill and ground in a tungsten mill until they achieve a D_{80} of 10 µm. The powdered samples were then split at Lisbon University until that a 20 g subsample was obtained, and then sent to the laboratory.

X-ray power diffraction of 14 waste rock samples from the stockpile was ran by SOMINCOR –through Escorsa Labs, resorting to a PANalytical X'pert PRO MPD, working with a Bragg–Brentano θ–θ geometry of 240 mm diameter, at a 45 kV voltage and a current of 40 mA; the machine is equipped with a CuKalpha radiation and operates with a divergent slit of 0.5°.

Semi-quantitative estimates of the mineral proportions in each sample obtained from XRD analyses through Rietveld method were combined with the geochemical data yielded by XRF, ICP-AES and ICP-MS, in order to provide the weight proportions of the various minerals present in the different samples per size fraction (*cf* [54].). This modal mineralogy was calculated for 515 samples using the GEO module of HSC Chemistry 10 software by Outotec. Error estimation of mass proportion of minerals in the samples was calculated using Monte Carlo Simulation with 200 iterations. All mass proportions were calculated using the Non-negative Least Square (NNLS) method. Nevertheless, it should be mentioned that, although quite robust and consistent, this approach to modal mineralogy cannot avoid the limitations arising from the fact that the mineral reference list for the various minerals was built on the basis of their stoichiometric compositions (*c.f.* Section 4.4) and not on their rigorous individual compositions measured sample by sample.

Acid Base Accounting and Net Acid Generation

*Acid base accounting (ABA) and net acid generation (NAG) t*ests were carried on for waste rock samples (SUL_NC_01 and SUL_NC_03) at AGQ Mining & Bioenergy laboratory in Spain. ABA tests included sulfur speciation using combustion-infrared TOC method, and Acid Potential (AP) and Neutralization Potential (NP) by using the Sobek test (Sobek et al., 1978) procedure, determined by reacting the sample with HCl, and back titrating with NaOH. Net Neutralization Potential (NNP), Neutralization Potential Ratio (NPR) and Net Acid Generation pH (NAGpH) were used to classify waste rock samples SUL_NC_01 and SUL_NC_03.

Net acid generation (NAG) tests were used to determine the balance between acid-producing and acid-consuming components of the waste rock using hydrogen peroxide to ensure oxidation of sulfides at different stages of the test. Acid produced by oxidation was consumed by carbonates and/or by other acid-consuming components of the waste rock samples. At the end of each stage, the sample is filtered to separate the solids from the NAG solution. The pH and acidity of the solution was then measured (NAG pH), while the solids were recovered to repeat oxidation using another dosage of hydrogen peroxide.

Results and Discussion

Particle Size Distribution

Considering the low proportion of fine particles passing the 1.25 mm mesh during coarse sieving (15.25% and 13.07% for SUL_NC_01 and SUL_NC_03, respectively), the fine sieving process was not enough to guarantee the representativity of the samples with a single sieving operation, implying its repetition for five times until we got a composite sample of waste rock passing through 1.25 mm mesh equivalent in weight to the ones used for coarse sieving.

Figure 6 graphically shows the particle size distribution for samples SUL_NC_01 and SUL_NC_03. The approximate values of D_{80} are 30 mm (30000 µm) for SUL_NC_01, and 22 mm (22000 µm) for SUL_NC_03, meaning that 80% of these materials pass through those sizes, respectively. In fact, although the materials were sieved "in situ", during the sampling campaign, the samples remained generally coarse.

The material over 4 mm represents (Table 2) 58.05% in the fresh waste rock (SUL_NC_01) and 56.94% in the old waste rock (SUL_NC_03), both having a similar particle size distribution, which reflects the fact that the underground crushing stage did not suffer significant modifications through time along mining operations.

Grain size distribution of tailings samples was obtained by laser diffraction analysis. Considering the disposal method used at Neves Corvo and the different uses given to the tailings, particle size distribution is not always homogeneous as seen with the waste rock. When backfill is carried on during mining operations only particles finer than 50 µm are pumped to the Cerro do Lobo TMF, which constrains the granulometry of the thickened tailings at the end of the process.

Samples taken directly from the Cerro do Lobo TMF, such as SUL_AGE_01T, SUL_AGE_02T, SUL_AGE_03T and SUL_AGE_04T, have an approximate D_{80} of 15 µm, while a sample taken at the last stream of the processing plants before being pumped to the Cerro do Lobo TMF (SUL_NC_02) that has a D_{80} of 40 µm (Fig. 7). The

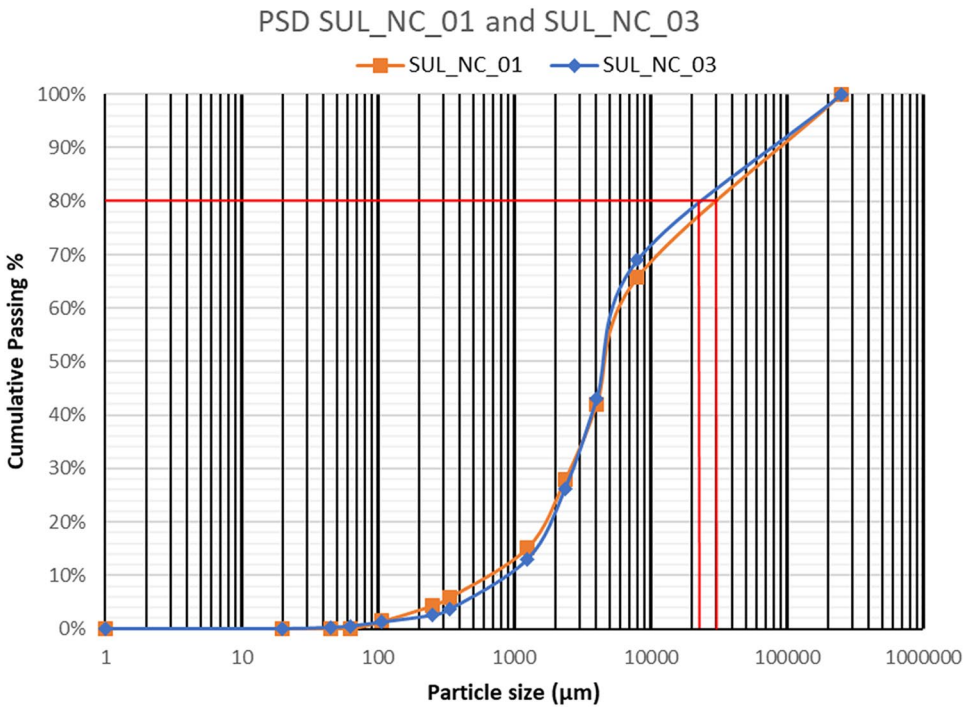

Fig. 6 Particle size distribution PSD for sample SUL_NC_01 and sample SUL_NC_03

Table 2 Cumulative weight retained coarse and fine sieving – samples SUL_NC_01 and SUL_NC_03

	Size (µm)	SUL_NC_01 Cum Weight %	SUL_NC_03 Cum Weight %
Material retained weight percentage	> 250,000	0.00%	0.00%
	> 8000	34.13%	30.96%
	> 4000	58.05%	56.94%
	> 2350	72.03%	73.80%
	> 1250	84.75%	86.93%
	> 335	94.07%	96.39%
	> 250	95.58%	97.45%
	> 106	98.54%	98.76%
	> 63	99.88%	99.48%
	> 45	99.96%	99.74%
	> 20	100.00%	99.98%
	> 1	100.00%	100.00%

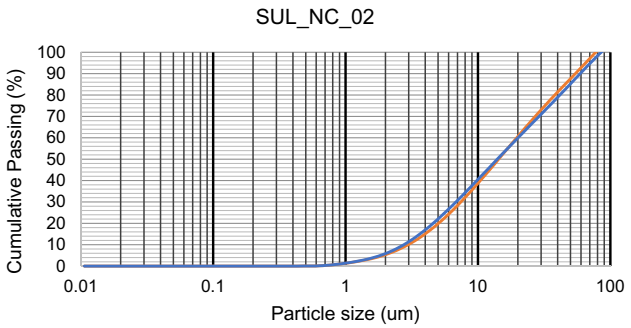

Fig. 7 Particle size distribution PSD from laser diffraction analysis in sample SUL_NC_02

latter sample was taken in the feeding valve to the hydrocyclones, prior to size separation (either to send the whole material to the thickener, or to split it in two fractions for backfilling and final disposal).

The particle sizes in the samples collected at the Cerro do Lobo TMF range between 1 and 30 µm, while the tailings collected at the last stream of copper and zinc processing plants, have particle sizes ranging between 1 and 100 µm.

Figure 8 shows the daily D_{80} variations of tailings collected at the last stream of the processing plants before disposal at the Cerro do Lobo TMF for a period of three months in 2019. The average value of D_{80} of tailings for the third trimester of 2019 is about 23.6 µm, which corresponds to a higher production of finer particles in the beneficiation

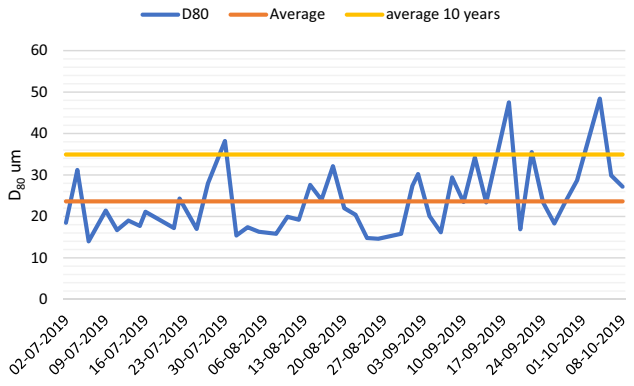

Fig. 8 D_{80} daily variations in the last tailings stream of the Neves Corvo processing plants before disposal at the Cerro do Lobo TMF (July to October 2019). Averages shown for comparison

process compared to the average value of D_{80} for the last 10 years, which is 34.9 µm (SOMINCOR, 2019).

Grindability Optimum Time

Three representative samples of each type of waste rock (SUL_NC_01 and SUL_NC_03) were ground at different times (15, 22.5 and 30 min). Each ground product was sieved in a ROTAP machine to get a particle size distribution in a size range between 1 and 10,000 µm (Fig. 9). Two values of D_{80} were considered for this analysis. The first value was extracted from the granulometric curve which represents experimental data, and the second value corresponds to a forecast based on a linear trend of the cumulative passing percentage values calculated.

In Fig. 10, the plots "time vs. D_{80}" for samples SUL_NC_01 and SUL_NC_03 were drawn both for experimental and theoretical values, and their corresponding linear regression trends were computed to obtain the line equation in the form $y = mx + b$, where "y" is the time required to achieve a certain value of "x" (D_{80}), "m" represents the gradient of the line, and "b" is a constant value (y-intercept). This approach provides the means to calculate the grindability optimum time for any particular size of particles. For instances, if the desired particle size for processing waste rock is 90 µm, as it is used for ore beneficiation at the processing plants of Neves Corvo, grindability optimum time would be 37 min for sample SUL_NC_01, and 33 min for sample SUL_NC_03. Shifts between the times obtained from experimental and theoretical approaches for both samples does not exceed 1%, which at laboratory and pilot plant scale does not represent a major variability. Upscaling of grindability optimum time for industrial use will however involve mill parameters that are not considered in this analysis.

Within the framework of the SULTAN project, optimum grindability time between 30 and 37 min was set at TU Clausthal, Germany, for grinding 200 kg of the two samples considered, aiming to prepare the material for pilot-scale sulfide flotation, in order to remove the sulfide fraction to produce a cleaner waste for industrial applications (ceramics, tiles, bricks, etc.). The achieved value of D_{80} felt between 85 and 90 µm, which was exactly what was expected (Fig. 11).

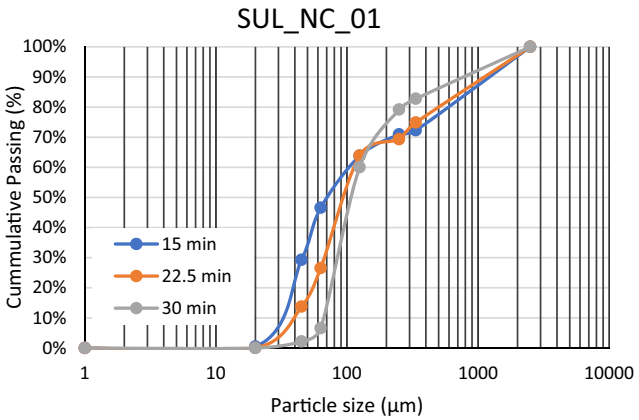

Time (min)	D_{80} experimental (µm)
15	600
22.5	500
30	250

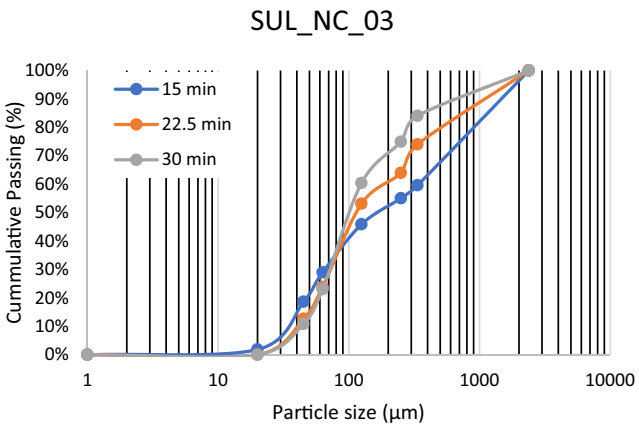

Time (min)	D_{80} experimental (µm)
15	900
22.5	500
30	290

Fig. 9 Cumulative curves after grinding times 15, 22.5, and 30 min with experimental D_{80} values for samples SUL_NC_01 and SUL_NC_03

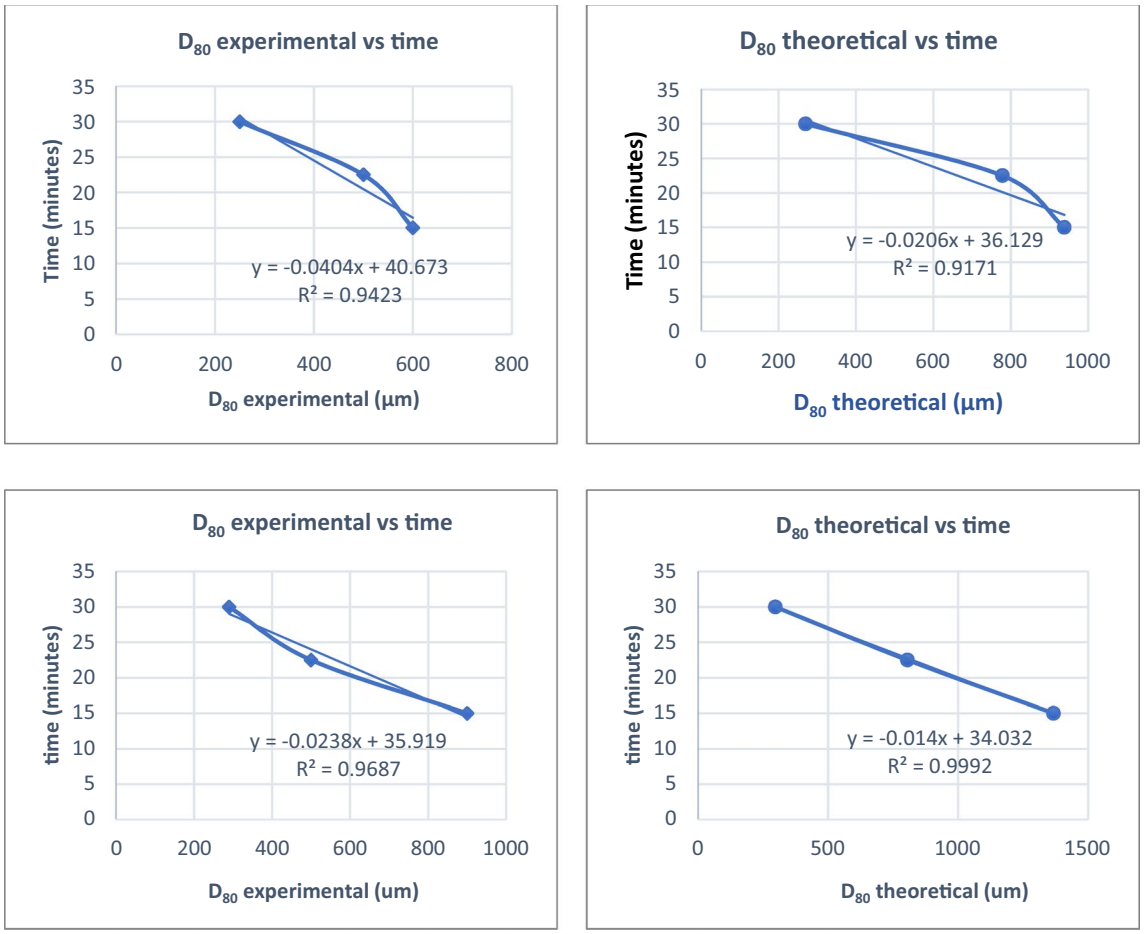

Fig. 10 Plot D_{80} vs time–linear regression; samples SUL_NC_01 (top) and SUL_NC_03 (bottom)

Geochemistry

Fresh and Old Waste Rock

Whole-rock geochemical analyses for samples SUL_NC_01, SUL_NC_02 and SUL_NC_03 measured by portable XRF were positively compared with corresponding data obtained at ALS Geochemistry, and XRF analyses performed at SOMINCOR's XRF laboratory (Fig. 5). A summary of XRF data is shown in Table 3. Waste rock samples composition is dominated by SiO_2 (42–55 wt%), Fe_2O_3(12–17 wt%) and Al_2O_3(9–14 wt%), with significant sulfur content, up to *ca.*5 wt% S, and low base metals contents (0.12–0.4 wt% Cu and 0.09–0.3wt% Zn). Tin and lead contents in waste rock samples do not surpass 600 ppm (133–537 ppm @Sn and 346–565 ppm @Pb), which precludes any possible interest in considering the recovery potential of these elements from waste rocks. In general terms, both materials (SUL_NC_01 and SUL_NC_03) have similar compositions regarding their major constituents; however, when it comes to a deleterious element such as arsenic it becomes quite clear that the altered material stored in the stockpile (SUL_NC_03; 1000–1020 ppm As) shows supergene enrichment relative to the fresh waste rock (SUL_NC_01; 466–472 ppm As), which obviously has relevant environmental implications.

Figure 12 shows the concentration of target elements by size fraction for SUL_NC_01. Values for copper and lead show little variation as a function of particle size distribution, except for a slight increase of copper grade in the fraction between 4 mm and 1.25 mm. Conversely, the trend of zinc contents along the different size fractions clearly shows two peak values: one in the coarser side of the granulometric curve (fraction 2.38 mm), and the other in its opposite side (fraction 20 µm). A possible interlocking of "zinc-bearing particles" in the coarser fraction and already liberated "zinc-bearing particles" in the finer fraction can possibly explain this trend as it will be investigated by detailed optical inspection, automated mineralogy, and Mineral Liberation Analysis (MLA) in the next stage of this on-going research.

The composition of sample SUL_NC_03 at the various size fractions (Fig. 13) shows a flat trend for lead that is similar to the one observed in fresh waste rock.

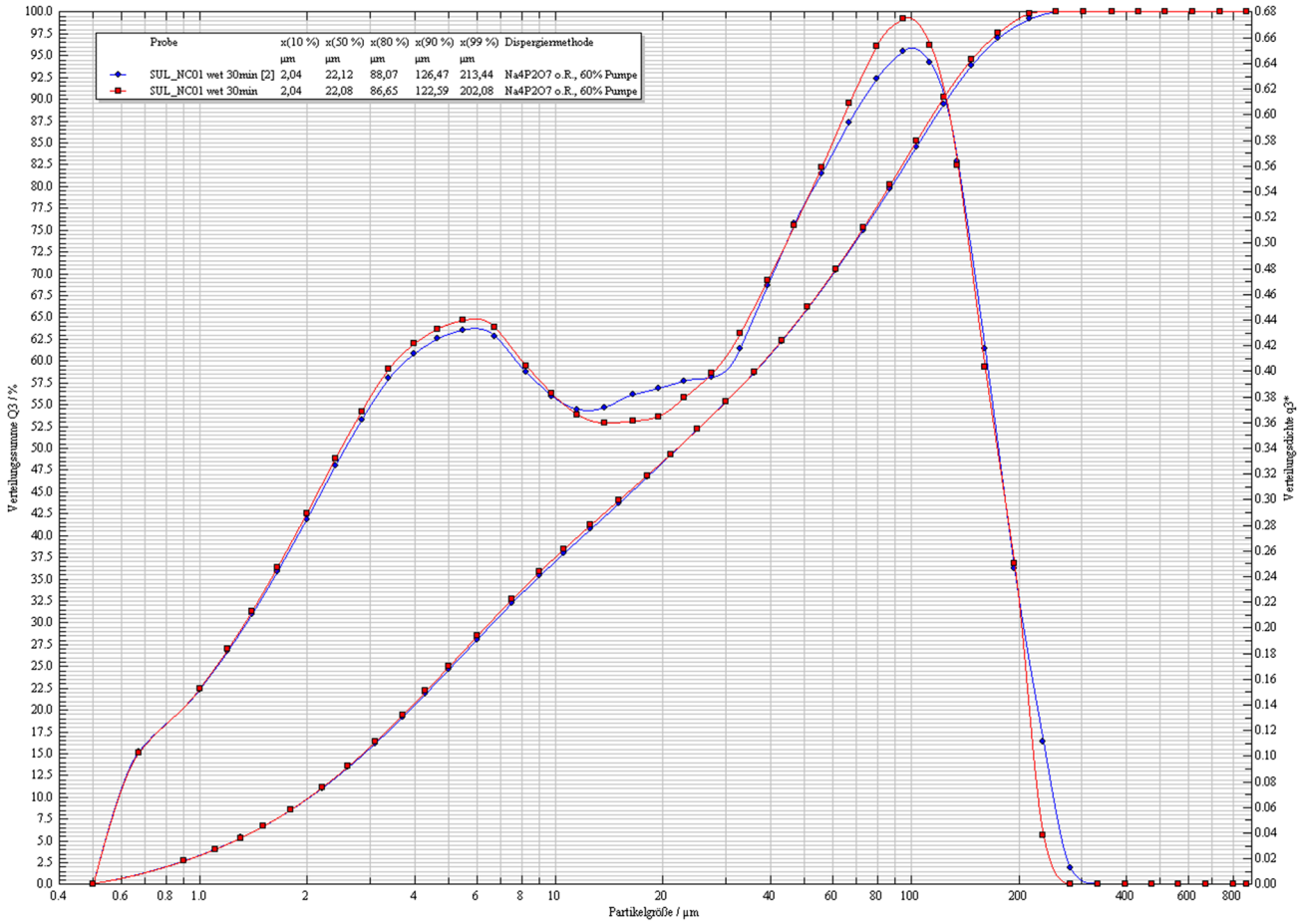

Fig. 11 Cumulative and non-cumulative particle size distribution of pilot-scale grinding for sample SUL_NC_01 at TU Clausthal (March 2020—SULTAN Project)

Table 3 Bulk chemistry of samples SUL_NC_01and SUL_NC_03 (summary)

ID	SiO_2_%	Al_2O_3_%	Fe_2O_3_%	K_2O_%	S_%
SUL_NC_01	51.19	9.68	15.63	2.61	4.98
SUL_NC_01	51.49	9.56	15.62	2.59	4.29
SUL_NC_01	55.31	13.50	16.97	2.12	4.99
SUL_NC_03	42.63	8.94	12.59	3.37	3.20
SUL_NC_03	42.92	9.08	12.52	3.37	3.18
SUL_NC_03	54.46	14.69	13.01	2.83	3.22
ID	Cu_%	Zn_%	Pb_ppm	As_ppm	
SUL_NC_01	0.12	0.30	565.73	472.08	
SUL_NC_01	0.12	0.30	565.37	460.65	
SUL_NC_01	0.17	0.36	805.00	466.37	
SUL_NC_03	0.33	0.12	346.41	1018.89	
SUL_NC_03	0.34	0.12	336.94	1011.41	
SUL_NC_03	0.43	0.09	365.00	1015.00	

However, it reveals significant differences relative to sample SUL_NC_01 regarding the behavior of copper and zinc.

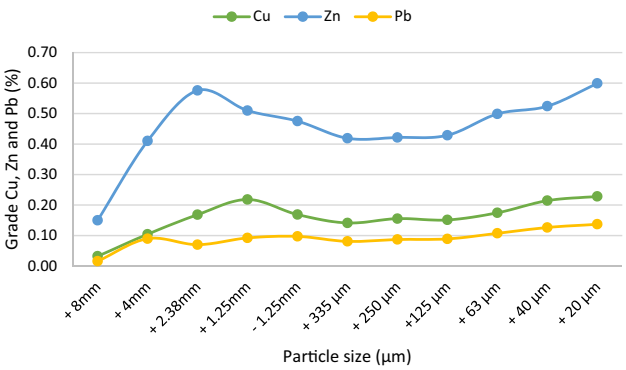

Fig. 12 Base metal contents of fresh waste rock (SUL_NC_01) as a function of size fraction

Differently from the fresh waste rock, where zinc content was higher than copper and variable along the granulometric curve, the oxidized sample SUL_NC_03 shows zinc depletion and a homogeneously low zinc distribution along size fractions. Instead, the copper content in this sample shows

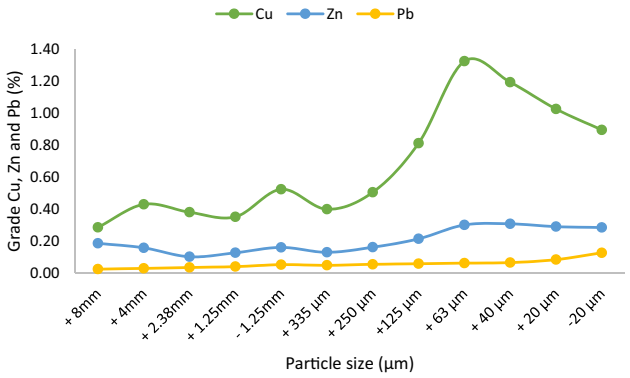

Fig. 13 Base metal contents of oxidized waste rock (SUL_NC_03) as a function of size fraction

a general copper enrichment relative to the fresh waste rock, which is particularly significant in the finer fractions, and especially in the particles sized between 335 µm and 63 µm. This copper behavior is most likely related with supergene enrichment of the old waste rock stockpile and secondary copper allocation to fine-grained alteration minerals.

The metal contents of samples SUL_NC_01 and SUL_NC_03 show values that might be potentially interesting for the possible reprocessing of these materials. However, as the D_{80} of both samples is in the millimetric range and considering that ore processing at beneficiation stage only uses sizes below 63 µm, crushing and grinding would be needed prior to any other processing stage. The composition of these waste rock residues does not preclude as well their potential for further use looking to other, non-metallic, industrial applications.

Layers in Waste Rock Stockpile

As it has been referred in Sect. 3.1.1 and shown in Fig. 3, the long exposure to weathering effects of the old waste rock stockpile led to formation of different layers of oxidized material showing contrasting colors. Samples representative of each of these colored layers were separately analyzed by XRF and the corresponding results are presented in Table 4. These results are particularly interesting when compared with the composition of the old waste rock material SUL_NC_03 above described, as the later represents in fact a mixed composite of the various layers (see sampling procedures in Sect. 3.1.1). The compositions of the different colored layers provide a means to better understand the chemical modifications related with the meteoric alteration suffered by the stockpile though time. In a way, the succession of colors, starting with the black layer (SUL_AGE_01W) and going through the reddish (SUL_AGE_05W), grayish (SUL_AGE_03W), yellowish (SUL_AGE_02W) and finally, the whitish layer (SUL_AGE_04W), illustrate a rough profile of supergene alteration. The black layer is for sure the one where pyrite (and other sulfides) is better preserved. Along the path composed by those four initial layers one can see the progressive decrease in iron and sulfur contents and variable metal leaching. In fact, it represents a copper(zinc)-enriched basal horizon where the above leached metals and sulfur do precipitate as secondary products, especially sulfates.

In samples SUL_AGE_01W (black layer), SUL_AGE_02W (yellow layer), SUL_AGE_03W (grayish layer) and SUL_AGE_05W (reddish layer) sulfur contents vary between 2.2 and 5.0 wt%. Whereas these four colored samples have as main constituents SiO_2 (39–45 wt%), Fe_2O_3 (10–20 wt%), and Al_2O_3 (7–12 wt%), consistently with the results of the old waste rock material above described (SUL_NC_03), sample SUL_AGE_04W (white layer) presents very low SiO_2 (3.8 wt%), Fe_2O_3 (1.6 wt%), and Al_2O_3 (2.1 wt%) contents, and a pronounced increase of the sulfur content (10.8 wt%), consistently with chemical precipitation and occurrence of sulfate minerals in this layer, accompanied by base metal enrichment (much higher values of Cu—1.3wt%—and Zn—1.0wt%).

Table 4 Bulk chemistry of samples SUL_AGE_01W(black layer), SUL_AGE_05W(reddish layer), SUL_AGE_03W(grayish layer), SUL_AGE_02W(yellow layer), and SUL_AGE_04W (white layer)

ID (top to bottom)	SiO2_%	Al_2O_3_%	Fe_2O_3_%	K_2O_%	S_%
SUL_AGE_01W (black layer)	42.726	11.727	20.111	2.258	5.021
SUL_AGE_05W (red layer)	39.622	7.013	18.422	1.964	3.444
SUL_AGE_03W (grayish layer)	45.096	9.274	13.261	2.799	3.796
SUL_AGE_02W (yellow layer)	41.853	7.734	10.601	2.858	2.290
SUL_AGE_04W (white layer)	3.805	2.053	1.602	0.264	10.754
ID (top to bottom)	Cu_%	Zn_%	Pb_ppm	As_ppm	Sn_ppm
SUL_AGE_01W (black layer)	0.564	1.847	1427.940	1567.920	353.460
SUL_AGE_05W (red layer)	0.458	0.078	172.040	694.950	433.850
SUL_AGE_03W (grayish layer)	0.269	0.182	153.870	638.040	239.890
SUL_AGE_02W (yellow layer)	0.245	0.086	195.370	347.910	241.490
SUL_AGE_04W (white layer)	1.345	1.028	15.750	124.300	22.730

Table 5 Bulk chemistry of sample SUL_NC_02 (summary)

ID	Cu_%	Zn_%	Fe_%	Pb_%	As_ppm	S_%
SUL_NC_02_1	0.35	0.93	25.55	0.31	5110.69	24.78
SUL_NC_02_2	0.35	0.95	25.29	0.31	4817.69	24.16
SUL_NC_02_3	0.33	0.79	25.72	0.30	4981.23	24.87
SUL_NC_02_4	0.31	0.80	25.56	0.31	5135.10	24.94
SUL_NC_02_5	0.31	0.89	25.45	0.30	4887.38	25.08
ID	SiO_2_%	Al_2O_3_%	K_2O_%	CaO_%		
SUL_NC_02_1	33.56	7.17	0.73	1.08		
SUL_NC_02_2	33.36	6.97	0.74	1.04		
SUL_NC_02_3	32.05	7.12	0.76	1.05		
SUL_NC_02_4	32.54	7.33	0.74	1.08		
SUL_NC_02_5	33.51	7.36	0.73	1.20		

Tailings

Sample SUL_NC_02 represents the tailings streams coming out of the processing plants before being mixed and sent to the Cerro do Lobo TMF tailings, *i.e.,* the non-valuable materials, thus the gangue minerals plus the valuable metals that were not able to be recovered during beneficiation process. Expectingly, tailings have as main constituents Fe (~ 26 wt%), SiO_2 (~ 33wt%) and sulfur (24–28 wt%), (Table 5) reflecting the mineralogical composition of the residue of the processing plants: pyrite, quartz, and phyllosilicates.

This study focuses on the recovery of valuable metals and by-products from sulfidic tailings. Grades of Zn (0.7–1.3 wt%), and Pb (0.3–0.7 wt%) might be interesting, whereas grades of Cu (0.3–0.6wt%) might be compared with primary ores of some deposits around the world (porphyry copper deposits), which makes Neves Corvo tailings a possible source of mineral resources by the end of the mine's operation. Other possible by-products in tailings, such as Sn (600–100 ppm), Sb (200–500 ppm), Ag (13–20 ppm) and Co (200–250 ppm), might be interesting in the future as well.

Considering the tailings samples collected on surface in three different sectors of the Cerro do Lobo TMF, which correspond to disposals made in October 2019, in March 2019, and in 2014, no significant compositional variations have been detected so far, with the exception of a slight reduction of SiO_2 (from 30 to 22 wt%) and a slight increase in iron (Fe) content (23 to 27 wt%) observed in samples from March 2014. The on-going drilling campaign (CPTu) at the Cerro do Lobo TMF will provide a complete set of samples that will allow the 4D (space–time) geochemical characterization of the Cerro do Lobo TMF tailings, which will be combined with historical data to build an integrated model for the tailings dam.

Mineralogy

Mineralogical analyses of fresh waste rock material (SUL_NC_01) by semi-quantitative XRD analysis (Fig. 14), revealed a mineral composition dominated by quartz (57.3%—SiO_2), Chlorite (chamosite (21,9%—$(Fe^{2+}, Mg)_5Al(AlSi_3O_{10})(OH)_8$)), biotite (2.4%—$K(Mg,Fe)_3(AlSi_3O_{10})(F,OH)_2$) and muscovite (16.4%—$KAl_2(AlSi_3)O_{10}(OH)_2$), with minor proportions of sulfides, such as pyrite (2.3%—FeS) and chalcopyrite (0.2%—$CuFeS_2$).

Other minerals, macroscopically identified in hand specimen, such as jarosite ($KFe^{3+}(SO_4)_2(OH)_6$), gypsum ($CaSO_4.2H_2O$) and plagioclase ($NaAlSi_3O_8$-$CaAl_2Si_2O_8$), were detected in much lower abundances.

XRD analyses performed at SOMINCOR's XRD laboratory for 14 sub-samples of oxidized waste rock stockpile, (SUL_NC_03) allowed the mineralogical characterization of the oxidized waste rock material stored in the stockpile (including the various colored layers). Table 6 summarizes the mineral phases identified and their approximate relative proportions.

The main mineral constituents of the oxidized waste rock stockpile (SUL_NC_03) are quartz (56.7%—SiO_2), muscovite (17.0%—$KAl_2(AlSi_3)O_{10}(OH)_2$), and chlorite (21.8—chamosite ($(Fe^{2+}, Mg)_5Al(AlSi_3O_{10})(OH)_8$) with minor proportions of pyrite (2.5%—FeS_2; only a few anomalous abundances above 10%), gypsum (2%—$CaSO_4{\cdot}2H_2O$), carbonates, and some minor additional silicate minerals. It is important to notice the recurrent occurrence of gypsum in this old waste rock material, resulting from the weathering of sulfides into sulfates, as it differentiates it from fresh waste rock where this mineral was not identified.

The semi-quantitative mineralogical XRD characterization of SUL_NC_02 (Fig. 15) has shown that quartz (30%—SiO_2), pyrite (43.1%—FeS_2) and chamosite (22.5%—$(Fe^{2+}, Mg)_5Al(AlSi_3O_{10})(OH)_8$), with very minor amounts of chalcopyrite (0.3%—$CuFeS_2$) and phyllosilicates (4.1%), are

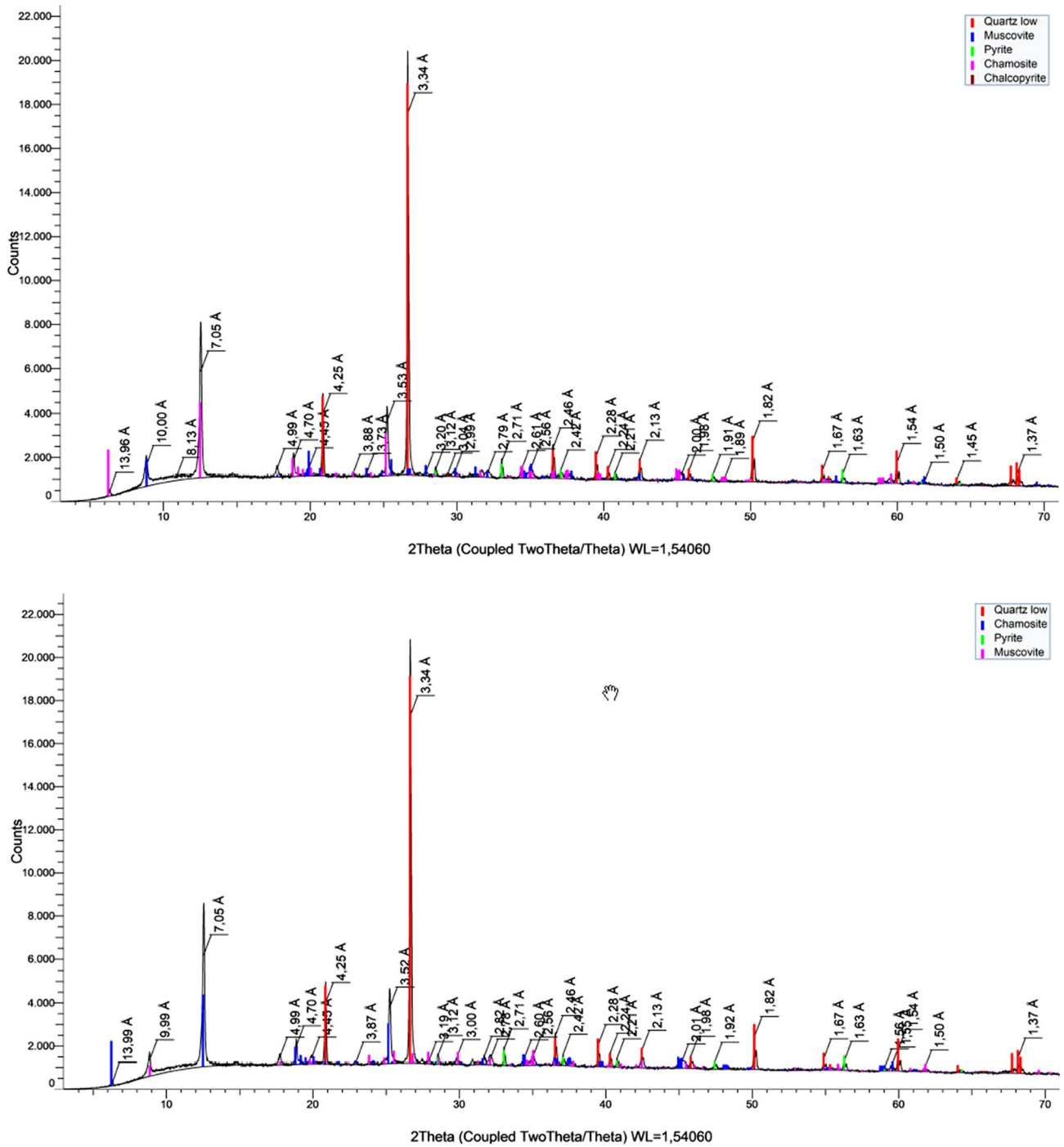

Fig. 14 Diffraction spectra of samples SUL_NC_01(top) and SUL_NC_03 (bottom) (fresh and oxidized waste rock)

largely predominant in the tailings stream of the processing plants.

It is known that XRD is much more accurate in measuring large and abundant crystalline structures rather than small and very minor ones. Therefore, it is likely that other minerals,, such as sphalerite (Fe,Zn)S), galena (PbS), tetrahedrite ($(Cu,Fe)_{12}Sb_4S_{13}$) and some carbonates, might have not been detected in the XRD spectra if occurring in very minor proportions or small crystalline phases.

Modal mineralogy, also known as element-to-mineral conversion, was also performed in order to add to our XRD mineralogy estimates, ground on an independent approach, of the mineral proportions present in the chemically analyzed samples. After testing different alternatives, a plausible

Table 6 Mineral proportions in sub-samples from the oxidized waste rock (SUL_NC_03)

X-ray diffraction (XRD) Analyses of Neves Corvo Waste Rock from the stockpile (SOMINCOR, 2019)								
Sample		Subsample 1	Subsample 2	Subsample 3	Subsample 4	Subsample 5	Subsample 6	Subsample 7
Quartz	%	50	51	63	56	53	47	44
Muscovite	%	42	34	7	34	31	45	42
Gypsum	%	2	2	3	2	2	1	1
Pyrite	%	2	3	20		1		4
Jarosite	%				3	4	2	
Clinoclhore	%	4	8	5		6	5	
Chamosite	%				5			8
Chalcopyrite	%			2				
Ankerite	%	0	2					
Braunite	%				< 1			
Bustamite	%					3		
Calcite	%							1
Sample		Subsample 8	Subsample 9	Subsample 10	Subsample 11	Subsample 12	Subsample 13	Subsample 14
Quartz	%	49	44	49	42	47	43	47
Muscovite	%	42	37	32	39	42	42	43
Gypsum	%	< 1	< 1	2	1	1	1	
Pyrite	%	2	12	3	9			2
Jarosite	%			2		2	3	
Clinoclhore	%	6					10	6
Chamosite	%		6	12	8	7		
Chalcopyrite	%				1			
Braunite	%					1	< 1	
Calcite	%	< 1	< 1					
Dolomite	%							2

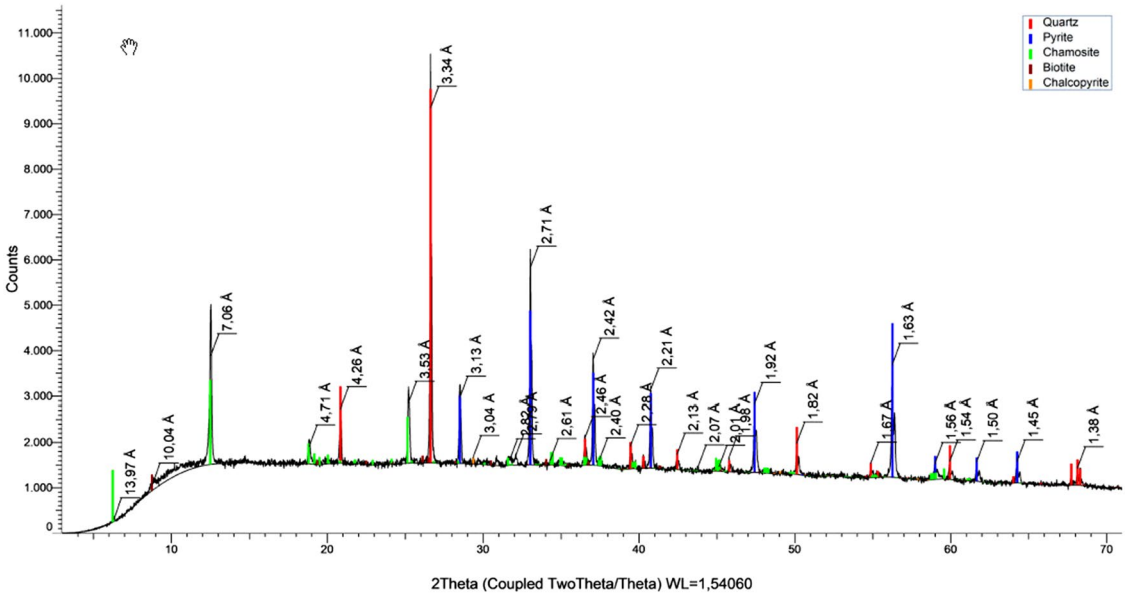

Fig. 15 Diffraction spectra for sample SUL_NC_02 (tailings)

Table 7 Mineral–mass proportion for sub-samples of the SUL_NC_01 (fresh waste rock) – (Sp-sphalerite, Ccp-chalcopyrite, Gn-Galena, Apy-Arsenopyrite, Ttrh-tetrahedrite, Stnn-stannite, Dol-Dolomite, Ms-Muscovite, Chms-chamosite, Py-pyrite and Qtz-Quartz)

ID	Sp %	Ccp %	Gn %	Apy %	Ttrh %	Stnn %	Dol %	Ms %	Chms %	Py %	Qtz %	Total
SUL_NC_01	0.479 ± 0.154	0.247 ± 0.094	0.071 ± 0.046	0.110 ± 0.075	0.035 ± 0.038	0.063 ± 0.059	2.871 ± 0.676	22.176 ± 2.897	8.297 ± 2.989	16.464 ± 3.262	39.092 ± 1.304	89.903 ± 6.090
SUL_NC_01	0.684 ± 0.197	0.283 ± 0.110	0.107 ± 0.066	0.167 ± 0.107	0.038 ± 0.044	0.071 ± 0.072	3.091 ± 0.739	15.009 ± 1.888	0.000 ± 0.000	23.333 ± 1.289	25.700 ± 0.884	68.480 ± 5.237
SUL_NC_01	0.608 ± 0.188	0.342 ± 0.114	0.095 ± 0.062	0.152 ± 0.104	0.042 ± 0.047	0.092 ± 0.085	2.029 ± 0.632	13.080 ± 1.860	0.000 ± 0.000	25.934 ± 1.456	31.826 ± 1.165	74.201 ± 5.567

Table 8 Mineral–mass proportion for sub-samples of the SUL_NC_03 (oxidized waste rock) – (Qtz-Quartz, Ms-Muscovite, Gy-Gypsum, Py-Pyirite, Ccp-Chalcopyrite, Jr-Jarosite, Cch-Clinoclhore, Chms-Chamosite, Ank-Ankerite, Dol-Dolomite, Sp-sphalerite, Gn-Galena, and Apy-Arsenopyrite,)

ID	Qtz %	Ms %	Gyp %	Py %	Ccp %	Jr %	Cch %	Chms %	Ank %	Dol %	Sp %	Gn %	Apy %	Total
SUL_NC_03	31.197 ± 0.936	19.302 ± 2.112	5.911 ± 0.726	0.255 ± 0.319	0.975 ± 0.324	11.806 ± 1.798	0.000 ± 0.002	10.956 ± 1.491	0.379 ± 0.728	0.006 ± 0.010	0.196 ± 0.106	0.045 ± 0.036	0.226 ± 0.129	81.254 ± 5.713
SUL_NC_03	35.750 ± 0.634	28.738 ± 2.072	3.228 ± 0.649	3.840 ± 0.097	1.257 ± 0.351	0.000 ± 0.000	3.960 ± 0.661	17.808 ± 0.977	0.000 ± 0.000	0.000 ± 0.000	0.158 ± 0.084	0.052 ± 0.038	0.171 ± 0.126	94.963 ± 5.586
SUL_AGE_01W (black layer)	26.402 ± 0.872	19.361 ± 2.508	1.364 ± 1.378	5.928 ± 0.674	1.567 ± 0.422	0.223 ± 0.508	2.751 ± 0.641	27.300 ± 0.934	0.000 ± 0.000	3.742 ± 2.390	3.023 ± 0.442	0.181 ± 0.088	0.330 ± 0.172	92.174 ± 6.416
SUL_AGE_05W (red layer)	29.345 ± 0.974	9.504 ± 1.822	0.324 ± 0.840	3.214 ± 0.432	1.305 ± 0.404	8.664 ± 1.163	2.119 ± 0.441	20.526 ± 0.540	0.000 ± 0.000	3.831 ± 1.610	0.107 ± 0.082	0.023 ± 0.024	0.130 ± 0.104	79.091 ± 5.947
SUL_AGE_03W (grayish layer)	32.947 ± 0.964	18.776 ± 2.190	0.463 ± 1.158	4.740 ± 0.616	0.765 ± 0.293	6.205 ± 1.329	1.796 ± 0.681	12.119 ± 0.707	0.000 ± 0.000	4.199 ± 1.831	0.269 ± 0.130	0.022 ± 0.022	0.113 ± 0.092	82.413 ± 5.846
SUL_AGE_02W (yellow layer)	31.973 ± 1.044	16.592 ± 2.103	0.368 ± 0.860	1.223 ± 0.388	0.734 ± 0.278	9.845 ± 1.505	1.052 ± 0.494	8.536 ± 0.780	0.026 ± 0.372	3.426 ± 1.582	0.144 ± 0.087	0.030 ± 0.027	0.082 ± 0.070	74.031 ± 5.601
SUL_AGE_04W (white layer)	0.979 ± 0.094	2.999 ± 0.642	10.367 ± 0.640	6.313 ± 0.208	4.105 ± 0.651	0.000 ± 0.000	4.391 ± 0.817	0.000 ± 0.000	0.000 ± 0.000	0.000 ± 0.000	3.644 ± 0.375	0.475 ± 0.025	0.000 ± 0.000	33.272 ± 3.121

Table 9 Mineral–mass proportion for sub-samples of the SUL_NC_02 (tailings) – (Sp-sphalerite, Ccp-chalcopyrite, Gn-Galena, Apy-Arsenopyrite, Ttrh-tetrahedrite, Stnn-stannite, Ms-Muscovite, Chms-chamosite, Py-pyrite and Qtz-Quartz)

ID	Sp %	Ccp %	Gn %	Apy %	Ttrh %	Stnn %	Ms %	Chms %	Py %	Qtz %	Total
SUL_NC_02_1	1.486 ± 0.458	0.508 ± 0.371	0.362 ± 0.341	1.107 ± 0.442	0.121 ± 0.127	0.367 ± 0.217	12.288 ± 2.004	12.087 ± 0.990	44.212 ± 1.742	24.943 ± 0.965	97.480 ± 5.767
SUL_NC_02_2	1.498 ± 0.421	0.465 ± 0.342	0.365 ± 0.313	1.045 ± 0.398	0.103 ± 0.110	0.360 ± 0.199	11.885 ± 1.857	12.509 ± 1.063	43.317 ± 1.621	25.138 ± 0.936	96.684 ± 5.433
SUL_NC_02_3	1.209 ± 0.408	0.452 ± 0.374	0.335 ± 0.329	1.063 ± 0.429	0.097 ± 0.115	0.324 ± 0.200	12.530 ± 1.977	11.669 ± 1.121	44.701 ± 1.763	23.433 ± 0.952	95.814 ± 5.642
SUL_NC_02_4	1.247 ± 0.415	0.418 ± 0.345	0.359 ± 0.337	1.121 ± 0.444	0.099 ± 0.115	0.332 ± 0.205	13.323 ± 2.037	11.533 ± 1.113	44.740 ± 1.754	23.641 ± 0.921	96.813 ± 5.603
SUL_NC_02_5	1.412 ± 0.509	0.433 ± 0.411	0.363 ± 0.376	1.078 ± 0.487	0.101 ± 0.129	0.345 ± 0.236	13.525 ± 2.282	10.774 ± 1.474	45.062 ± 2.037	24.764 ± 1.065	97.857 ± 6.418

Table 10 Average values of sulfur speciation for SUL_NC_01 and SUL_NC_03 sub-samples

SUL_NC_01-average		SUL_NC_03-average	
Sulfur speciation	Value (%)	Sulfur speciation	Value (%)
S_{total}	4.87	S_{total}	3.95
Sulfates	0.97	Sulfates	1.40
Sulfides	3.91	Sulfides	2.55

mineral conversion assessment for samples and sub-samples of SUL_NC_01, SUL, NC_02 and SUL_NC_03 was found. The GEO module of HSC Chemistry 10 software by Outotec, which involves three calculation rounds with Non-negative Least Square (NNLS) algorithm, was adopted. The first round included sulfides (except pyrite) and minerals which could be estimated based on one single element; a second round with minerals belonging to the classes of silicates (except quartz) and carbonates; and a third round with pyrite and quartz (as main gangue minerals). Table 7, Table 8, and Table 9, show the mineral proportions per sample plus/minus the standard deviation estimated by running Monte Carlo simulation with 200 iterations. It is important to mention that it was chosen not to normalize the mass proportions to a total of 100% in order to prevent hiding the possible occurrence of minor minerals (silicates gangue) that might be missing in the general list of minerals used. The tables displayed show that the modal mineralogy estimated fully confirm the XRD semi-quantitative characterization above presented: quartz, muscovite, and chamosite are largely predominant in the waste rock material (SUL_NC_01 and SUL_NC_03), whereas pyrite, quartz, and phyllosilicates are predominant in the tailings material (SUL_NC_02).

As mentioned in Sect. 4.3.2, the white layer (sample SUL_AGE_04W; Table 8) is not representative of the whole stockpile, since it corresponds to a bottom layer that only appears in areas where pronounced precipitation of sulfates occurred at the base of the pile. The gypsum content in this sulfate-rich layer more than doubles the average value for the stockpile shown by sample SUL_NC_03. The uncommonly low total shown by sample SUL_AGE_04W in Table 8 turns it clear how the set of minerals listed for the remaining samples is unsuitable to describe the modal mineralogy of this particular sample.

Acid Base Accounting and Net Acid Generation

There are several combinations of methods as part of the state of the art for the prediction and control of drainage chemistry such as monitoring data, field kinetic tests, laboratory kinetic tests, retention tests, mineralogy, total metals and whole rock analysis, and acid base accounting [55]. As already mentioned, at the Neves Corvo mine, the method

Table 11 Summary of ABA and NAG test results – waste rock samples

SUL_NC_01 Avg			SUL_NC_03 Avg		
Acidic potential (AP)	122.00	$kgCaCO_3/t$	Acidic potential (AP)	79.75	$kgCaCO_3/t$
ABA (neutralizing potential) Sobek method	9.16	$kgCaCO_3/t$	ABA (neutralizing potential) Sobek method	0.25	$kgCaCO_3/t$
pH paste	4.27		pH paste	4.27	
NAG (pH 4.5)	48.9	kgH_2SO_4/t	NAG (pH 4.5)	25.0	kgH_2SO_4/t
NAG (pH 7.0)	67.1	kgH_2SO_4/t	NAG (pH 7.0)	39.3	kgH_2SO_4/t
NAGpH	2.36		NAGpH	2.55	

developed by SOMINCOR for the disposal of tailings at Cerro do Lobo TMF by co-deposition with waste rock is aimed at guaranteeing the best conditions for the geochemical and geotechnical stability of the tailings dam. By avoiding the contact between the mine residues and water and air, it is intended to prevent oxidation and, consequently, the harmful effects of possible associated acid mine drainage. Waste rock stockpiles are kept in the industrial complex before its disposal at Cerro do Lobo TMF, with controlled drainage systems that prevent percolation of waters to the soil.

Two different tests—Acid Base Accounting (ABA) and Net Acid Generation (NAG) – were applied on six sub-samples of fresh (SUL_NC_01) and old waste rock (SUL_NC_03). Mine waste rocks in Neves Corvo, both old and fresh, consist of variably altered and mineralized silicate rocks—mostly felsic volcanic rocks, and/or siliceous metasediments—in variable proportions. However, although the main constituents (> 70%) of these materials are quartz, chamosite,, muscovite and some carbonates, there is still a variable percentage (5–20%) of disseminated sulfides such as pyrite, chalcopyrite, ± sphalerite and ± arsenopyrite, among other minor sulfide minerals, which could lead to potential generation of acid mine drainage. As expected, there is a slight difference in sulfur speciation between fresh (SUL_NC_01) and oxidized waste rocks (SUL_NC_03). Sub-samples of SUL_NC_01 show higher concentration of sulfur and larger proportion of sulfide minerals, while sub-samples of SUL_NC_03 show a decrease in sulfur concentrations, but a larger proportion of sulfates (Table 10). This difference obviously reflects the oxidation of sulfide minerals in the stockpile, with emphasis on pyrite (*ca.* 20% pyrite in SUL_NC_01 *versus ca.* 9% pyrite in SUL_NC_03), and re-precipitation of sulfur under the form of sulfate minerals such as jarosite, gypsum, among others. As it is common in VMS deposits, pyrite is by far the mineral with the largest potential for AMD generation in Neves Corvo.

The ABA and NAG results obtained in the course of this study are summarized in Table 11. Net neutralization potential (NNP) and Neutralization Potential Ratio (NPR) for the Neves Corvo waste rock samples were calculated based on the results obtained from ABA tests. Net Neutralization Potential (NNP) corresponds to the difference between neutralization potential (NP) and acid production potential (AP), while the Neutralization Potential Ratio is the ratio between NP and AP [56]. Materials are classified as acid producing if NNP is less than − 20 kg $CaCO_3$/t, non-acid producing if NNP greater than 20 kg $CaCO_3$/t and considered uncertain if NNP value is between − 20 and 20 kg $CaCO_3$/t. For NPR, it is considered that values of NPR < 1 are to produce AMD and values of NPR > 2 are to prevent AMD [55, 57, 58].

$$NNP = NP - AP$$

$$AvgNNP_{SUL\_NC\_01} = 9.16 - 122 \quad \mathrm{kgCaCO_3}/t$$

$$AvgNNP_{SUL\_NC\_03} = 0.25 - 79.75 \quad \mathrm{kg}CaCO_3/t$$

$$AvgNNP_{SUL\_NC\_01} = -112.84\mathrm{kg\ CaCO_3}/\boldsymbol{t}$$

$$AvgNNP_{SUL\_NC\_03} = -79.50\mathrm{kg\ CaCO_3}/\boldsymbol{t}$$

$$NPR = NP/AP$$

$$NPR_{SUL\_NC\_01} = 9.16/122 \quad NPR_{SUL\_NC\_03} = 0.25/79.75$$

$$NPR_{SUL\_NC\_01} = 0.075 \quad NPR_{SUL\_NC\_03} = 0.003$$

Both samples SUL_NC_01 and SUL_NC_03 should be classified as acid producing materials since their average NNP values (− 112.84 kg $CaCO_3$/t and − 79.5 kg $CaCO_3$/t, respectively) are clearly below the established limit. For Neves Corvo waste rock samples, the values of NPR are < 1 (0.075 for SUL_NC_01 and 0.003 for SUL_NC_03), confirming that both of them are considered as potential generators of AMD.

NAG test is a valuable quantitative proxy to the potential for net acid generation of a mine residue, especially when coupled with the results obtained for ABA tests [55]. NAGpH values below 4.5 indicate the material is potentially

acid generating, whereas NAGpH values equal or higher than 4.5 mean that the material is potentially net acid neutralizing. NAGpH values for samples SUL_NC_01 and SUL_NC_03 confirm the indications previously given by their net neutralizing potential—NNP. The NAGpH values obtained for samples SUL_NC_01 and SUL_NC_03 were 2.36 and 2.55 (Table 11), respectively, which is very much consistent with these mine waste rocks being potential acid-generating materials.

Conclusion

Neves Corvo mine produces two types of residues: waste rock and tailings. By using a sub-aerial disposal method in co-deposition with waste rock, Cerro do Lobo TMF has stored, between 2010 and 2019, 17 Mt of thickened tailings and 7.3 Mt of waste rock. In addition, 3.1 million tons of waste rock remained in a temporary stockpile at the mining complex. Tailings contain significant concentrations of valuable metals. Particle size analysis confirmed the fine grade of these residues and the challenge they represent for possible reprocessing and future mining. Grades of copper (0.3–0.6 wt%) and zinc (0.7–1.3 wt%) suggest them as the main target elements to recover. Mineral phases identified in the tailings samples are dominated by pyrite (FeS) and quartz (SiO_2), accompanied by other sulfides such as sphalerite, chalcopyrite, and galena, silicate minerals such as chlorite (clinochlore and chamosite) and plagioclase, and a minor proportion of carbonates. An on-going drilling campaign at Cerro do Lobo TMF and further studies at the resulting samples will allow us to characterize in depth the mineral associations, grade variability, and speciation of by-products for modeling and resource estimation.

Waste rock material is characterized for having a granulometric distribution toward the coarse (millimetric) fraction. However, when material was analyzed separately in different size ranges it was possible to observe the variability of valuable elements (Cu, Zn) according to size classification, which could lead to possible metal recovery and additional valorization of gangue residues—their main constituents (42–55% SiO_2, 9–15% Al_2O_3 and 12–17% Fe_2O_3) , as aggregates and/or construction raw materials. Similar mineralogy was identified for both fresh and oxidized waste rock (quartz, chamosite, pyrite); however, the mineral composition of oxidized waste rock includes additional phases that result from weathering reactions, such as jarosite, gypsum, ankerite, among others.

Acknowledgements We are grateful to all people taking part at the tailings and waste rock department and processing plants laboratories at SOMINCOR-Lundin Mining. Special thanks to Ana Rodrigues, Hugo Alves, Jorge Curral, Fábio Silva, and Rita Santos for all their contributions during sampling campaigns at Neves Corvo mine and for the data provided to the development of this study. This research was funded by the European Union's EU Framework Program for Research and Innovation Horizon 2020 under Grant Agreement No 812580, Project "MSCA-ETN SULTAN", and this publication is supported by FCT- Project UID/GEO/50019/2019—Instituto Dom Luiz. The text reflects only the authors' opinions, exempting EU Commission from any liability.

Declarations

Conflict of interest On behalf of all authors, the corresponding author states that there is no conflict of interest.

References

1. Carvalho J, Diamantino C, Rosa C, Carvalho E (2016) Potential recovery of mineral resources from mining tailing of abandoned mines in Portugal. In: Proceedings of the 3rd international symposium on enhanced landfill mining, Lisbon, Portugal, 8–10, pp 501–516
2. Martins L P (2012) Mineral resources of Portugal. Direcção Geral de Energia e Geologia. DGEG, Lisbon, pp 1–74
3. EDM - Empresa de Desenvolvimento Mineiro, DGEG (2011) The legacy of abandoned mines: the context and the action in Portugal. EDM
4. Sanchez España J (2008) Acid mine drainage in the Iberian Pyrite Belt : an overview with special emphasis on generation mechanisms aqueous composition and associated mineral phases. Rev Soc Eespañ Mineralog 10:34–43
5. Žibret G, Lemiere B, Mendez AM, Cormio C, Sinnett D, Cleall P, Szabo K, Carvalho T (2020) National mineral waste databases as an information source for assessing material recovery potential from mine waste, tailings and metallurgical waste. Minerals 10:1–20
6. Lottermoser BG (2010) Mine wastes (third edition): characterization, treatment and environmental impacts, pp 1–400
7. BRGM (2001) Management of mining, quarrying and ore-processing waste in the European Union, 79p, 7 Figs., 17 Tables, 7 annexes, 1 CD-ROM (Collected data)
8. DHI Environment (2007) Classification of mining waste facilities: fFinal report, p 207
9. Vallero DA, Blight G (2019) Chapter 6: Mine waste: a brief overview of origins, quantities, and methods of storage. In: Letcher TM, Vallero DA (eds) Waste, 2nd edn. Academic Press, New York, pp 129–151
10. Perreault NN, Mckinnell RJ, Delisle S (2015) Tailings, managing for the future. In: Proceedings tailings and mine waste conference. Vancouver, BC
11. Schoenberger E (2016) Environmentally sustainable mining: The case of tailings storage facilities. Resour Policy 49:119–128. https://doi.org/10.1016/j.resourpol.2016.04.009
12. Araya N, Kraslawski A, Cisternas LA (2020) Towards mine tailings valorization: recovery of critical materials from Chilean mine tailings. J Clean Prod 263:121–555
13. Eurostats (2021) Eurostats Data Browser. https://ec.europa.eu/eurostat/databrowser/view/ten00106/default/table?lang=en. Accessed 26 Apr 2021
14. Adiansyah JS, Rosano M, Vink S, Keir G (2015) A framework for a sustainable approach to mine tailings management: disposal strategies. J Clean Prod 108:1050–1062
15. Blengini GA, Mathieux F, Mancini L, Nyberg M, Cavaco Viegas H, Salminen J, Garbarino E, Orveillion G, Saveyn H (2019) Recovery of critical and other raw materials from mining waste

and landfills: state of play on existing practices. EUR 29744 EN, Publications Office of the European Union, Luxembourg. https://doi.org/10.2760/174367
16. Mehta N, Dino GA, Passarella I, Ajmone-Marsan F, Rossetti P, de Luca DA (2020) Assessment of the possible reuse of extractive waste coming from abandoned mine sites: case study in Gorno, Italy: Sustainability (Switzerland), vol 12, pp 1–22
17. Lomberg K, Rupprecht SM (2017) The SAMREC code. J S Afr Inst Min Metall 117:1095–1100
18. CRIRSCO (2019) The CRIRSCO International Reporting Template 2019. http://www.crirsco.com/template.asp. Accessed Jun 2020
19. Aznar-Sánchez JA, García-Gómez JJ, Velasco-Muñoz JF, Carretero-Gómez A (2018) Mining waste and its sustainable management. Advances in worldwide research: Minerals, v. 8
20. SULTAN (2018) European Training Network for the remediation and reprocessing of sulfidic mining waste sites: General proposal. European Comission Horizon 2020
21. Tailpro. (2021) https://www.tailings.info/basics/tailings.htm. Accessed on 23 Mar 2021
22. Relvas JMSR, Barriga FJAS, Pinto AMM, Ferreira A, Pacheco N, Noiva P, Barriga G, Baptista R, Carvalho D, Oliveira V, Munhá J, Hutchinson RW (2002) The Neves Corvo deposit, Iberian Pyrite Belt, Portugal: Impacts and future 25 years after the discovery. SEG Special Publication, Tulsa, pp 155–176
23. Lundin Mining (2021) Mineral Resources and Reserves - June 30, 2020. https://www.lundinmining.com/news/lundin-mining-announces-2020-mineral-resource-and-123002/ Accessed 30 Sept 2020
24. Lundin Mining (2020) Lundin Mining - Neves Corvo. Retrieved from Lundin Mining - Neves Corvo: https://www.lundinmining.com/operations/neves-corvo/. Accessed 1 Jun 2020
25. Wardell Armstrong International WAI (2017) NI 43-101 Technical Report for the Neves-Corvo Mine, Portugal
26. Wardell Armstrong International WAI (2007) Technical Report on the Neves Corvo Mine, Southern Portugal
27. Wardell Armstrong International WAI (2013) NI 43-101 Technical Report for Neves-Corvo Mine and Semblana Deposit, Portugal, January 2013, p 224
28. Gaspar OC (2002) Mineralogy and sulfide mineral chemistry of the neves-corvo ores, Portugal: Insight into their genesis. Can Mineralog 40:611–636
29. Relvas JMRS, Barriga FJAS, Ferreira A, Noiva PC, Pacheco N, Barriga G (2006) Hydrothermal alteration and mineralization in the neves-corvo volcanic-hosted massive sulfide deposit, Portugal: I Geology, mineralogy, and geochemistry. Econ Geol 101:753–790
30. Barriga FJAS (1990) Metallogenesis in the Iberian Pyrite Belt. In: Dallmeyer RD, Martinez García E (eds) Pre-Mesozoic geology of Iberia. Springer, Berlin, pp 369–379
31. Leistel JM, Marcoux E, Thiéblemond D, Quesada C, Sánchez A, Almodóvar GR, Pascual E, Sáez R (1998) The volcanic-hosted massive sulphide deposits of the Iberian pyrite belt. Mineral Depos 33:2–30
32. Carvalho D, Barriga FJAS, Munhá J (1999) Bimodal-siliciclastic systems: the case of the Iberian pyrite belt. Rev Econ Geol 8:375–408
33. Sáez R, Pascual F, Toscano M, Almodóvar JR (1999) The Iberian type of volcano-sedimentary massive sulfide deposits. Mineral Depos 34:549–570
34. Tornos F (2006) Environment of formation and styles of volcanogenic massive sulfides: the Iberian Pyrite Belt. Ore Geol Rev 28:259–307
35. Moura A (2008) Metallogenesis at the Neves Corvo VHMS deposit (Portugal): a contribution from the study of fluid inclusions. Ore Geol Rev 34:354–368
36. Barrie CT, Amelin Y, Pascual E (2002) U-Pb Geochronology of VMS mineralization in the Iberian Pyrite Belt. Mineral Depos 37:684–703
37. Rosa CJP, McPhie J, Relvas JMRS, Pereira Z, Oliveira T, Pacheco N (2008) Facies analyses and volcanic setting of the giant Neves Corvo massive sulfide deposit, Iberian Pyrite Belt, Portugal. Mineral Depos 43:449–466
38. Oliveira JT, Pereira Z, Carvalho P, Pacheco N, Korn D (2004) Stratigraphy of the tectonically imbricated lithological succession of the Neves Corvo mine area Iberian Pyrite Belt, Portugal. Mineral Depos 39:422–436
39. Solá AR, Salgueiro R, Pereira Z, Matos JX, Rosa CJP, Araújo A, Neto R, Lains JA (2015) Time span of the volcanic setting of the Neves-Corvo VHMS deposit. In: X Congresso Ibérico de Geoquímica, Lisboa, 19–23 Outubro 2015, pp 122–125
40. Relvas JMRS, Tassinari CCG, Munhá J, Barriga FJAS (2001) Multiple sources for ore-forming fluids in the Neves-Corvo VHMS deposit of the Iberian pyrite belt (Portugal): strontium, neodymium and lead isotope evidence. Mineral Depos 36:416–427
41. Relvas JMRS, Barriga FJAS, Longstaffe FJ (2006) Hydrothermal alteration and mineralization in the Neves-Corvo volcanic-hosted massive sulfide deposit, Portugal. II. Oxygen, hydrogen, and carbon isotopes. Econ Geol 101:791–804
42. Huston DL, Relvas JMRS, Gemmell JB, Drieberg S (2011) The role of granites in volcanic-hosted massive sulphide ore-forming systems: an assessment of magma-tic–hydrothermal contributions. Mineral Dept 46:473–507. https://doi.org/10.1007/s00126-010-0322-7
43. Carvalho JRS, Relvas JMRS, Pinto AMM, Frenzel M, Krause J, Gutzmer J, Pacheco N, Fonseca R, Santos S, Caetano P, Reis T, Gonçalves M (2018) Indium and Selenium distribution in the Neves-Corvo deposit Iberian Pyrite Belt, Portugal. Mineral Mag 82:S5–S41
44. Li X, Zhao K-D, Jiang S-Y, Palmer MR (2019) In-situ U-Pb geochronology and sulfur isotopes constrain the metallogenesis of the giant Neves-Corvo deposit, Iberian Pyrite Belt. Ore Geol Rev 105:223–235
45. Marques AFA, Relvas JMRS, Scott SD, Rosa C, Guillong M (2020) Melt inclusions in quartz from felsic volcanic rocks of the Iberian Pyrite Belt: clues for magmatic ore metal transfer towards VMS-forming systems. Ore Geol Rev 126:103743. https://doi.org/10.1016/j.oregeorev.2020.103743
46. Gaspar O, Pinto A (1991) The ore textures of the Neves Corvo volcanogenic massive sulphide and their implications for ore beneficiation. Mineral Mag 55:417–422
47. Pinto A, Bowles JFW, Gaspar OC (1994) The mineral chemistry and textures of wittichenite, miharaite, carrolite, mawsonite and In-Bi-Hg tennantite from Neves-Corvo, Portugal [abs]. In: Proceedings of the XVI general meeting of IMA, Pisa, Italy, p 329
48. Pinto A, Relvas JMRS, Barriga FJAS, Munhá J, Pacheco N, Scott SD (2005) Gold mineralization in recent and ancient volcanic-hosted massive sulphides: the PACMANUS field and the Neves-Corvo deposit. In: Mao J, Bierlein FP (eds) Mineral Deposit Research: meeting the global challenge, vol 1. Berlin. Germany, Springer-Verlag, pp 683–686
49. Pinto A., Bowles JFW, Benzaazoua M, Marion P, Ferreira A, Barriga FJAS (2004) Gold mineralization at the Neves Corvo ore deposit, Portugal. In: 32nd International Geological Congress, Florence
50. Rodrigues HE (2016) Mina de Neves-Corvo: Deposição de rejeitado espessado Acompanhamento geotécnico e geoquímico
51. Oliveira M (2019) Gestão de residuos mineiros Neves Corvo mine. Universidade de Lisboa, Palestra Faculdade de Ciencias
52. Real F, Franco A (1990) Tailings disposal at Neves Corvo Mine, Lisboa , Portugal, pp 209–221

53. Melo T (2015) Study of the influence of flocculation parameters on the tailings thickening process of Neves-Corvo Mine. Universidade Tecnica de Lisboa, Mestrado de Engenharia Geologica e de Minas. Instituto Superior Tecnico
54. Whiten B (2007) Calculation of mineral composition. Mineral Processing and Extractive Metallurgy Review, v. 7508
55. Morin KA, Hutt NM (1997) Environmental geochemistry of minesite drainage: practical theorynag and case studies. MDAG, Vancouver
56. Fey DL (2003) Acid-base accounting. In: Billings symposium/ASMR annual meeting. USGS
57. Miller SD, Jeffery JJ, Wong JWC (1991) Use and misuse of the acid-base account for "AMD" prediction. In: Proceedings of the 2nd international conf on the abatement of acidic drainage, Montreal, Canada, vol 3, CANMET, Ottawa, pp 489–506
58. Morin KA, Hutt NM (1994a) Observed preferential depletion of neutralization potential over sulfide minerals in kinetic tests: site-specific criteria for safe NP/AP ratios. In: Proceedings of the third international conference on the abatement of acidic drainage, Pittsburgh, Pennsylvania, USA, April 24–29, vol 1, pp 148–156